Distribution Category:
Magnetic Fusion Energy
(UC-20)

ANL/FPP/TM--208

DE87 005583

ANL/FPP/TM-208

ARGONNE NATIONAL LABORATORY
9700 South Cass Avenue
Argonne, Illinois 60439

DESIGN ANALYSES OF SELF-COOLED LIQUID METAL BLANKETS

by

Y. Gohar

Fusion Power Program

December 1986

Work supported by

Office of Fusion Energy
U.S. Department of Energy

TABLE OF CONTENTS

		Page
ABSTRACT		1
I.	Introduction	2
II.	Parametric Studies	3
	II.1 Tritium Breeding	3
	II.2 Blanket Energy Multiplication	10
	II.3 Shield Energy Deposition	17
	II.4 Optimum Design Parameters for the Liquid Metal Blanket Concepts	22
III.	Impact of Reactor Design Choices on the Performance Parameters	24
	III.1 Computational Models	24
	III.2 Tritium Breeding and Energy Deposition Changes	27
IV.	Tritium Breeding Benchmark Calculations for Liquid Lithium Blankets	33
References		41

LIST OF FIGURES

Number		Page
1.	Tritium breeding ratio as a function of the carbon reflector zone thickness for different lithium-lead breeding zone thicknesses with natural lithium enrichment	7
2.	Tritium breeding ratio as a function of the steel reflector zone thickness for different lithium-lead breeding zone thicknesses with natural lithium enrichment	8
3.	Tritium breeding ratio as a function of the steel reflector zone thickness for different lithium-lead breeding zone thicknesses with 90% lithium-6 enrichment	9
4.	Tritium breeding ratio as a function of the lithium-lead breeding zone thickness for different steel reflector zone thicknesses with 30% lithium-lead enrichment	11
5.	Tritium breeding ratio as a function of the lithium-lead breeding zone thickness for different steel reflector zone thicknesses with 90% lithium-6 enrichment	12
6.	Tritium breeding ratio as a function of the lithium breeder zone thickness for different steel reflector zone thicknesses with natural lithium enrichment	13
7.	Blanket energy multiplication factor as a function of the lithium-lead zone thickness for different steel reflector zone thicknesses with 30% lithium-6 enrichment	15
8.	Blanket energy multiplication factor as a function of the lithium-lead zone thickness for different steel reflector zone thicknesses with 90% lithium-6 enrichment	16
9.	Blanket energy multiplication factor as a function of the lithium breeder zone thickness for different steel reflector zone thicknesses with natural lithium enrichment	18
10.	Fraction of the total energy deposited in the shield as a function of the lithium-lead breeder zone thickness for different steel reflector zone thicknesses with 30% lithium-6 enrichment	19

LIST OF FIGURES (cont'd)

Number		Page
11.	Fraction of the total energy deposited in the shield as a function of the lithium-lead breeder zone thickness for different steel reflector zone thicknesses with 90% lithium-6 enrichment.....	20
12.	Fraction of the total energy deposited in the shield as a function of the lithium breeder zone thicknesses for different steel reflector zone thicknesses with natural lithium enrichment.....	21
13a.	Reactor geometrical model with a tritium breeding blanket for both inboard and outboard sections.....	28
13b.	Reactor geometrical model with an outboard tritium breeding blanket and an outboard steel blanket.....	28
13c.	Reactor geometrical model with a tritium breeding blanket for both the inboard and outboard sections with a bottom limiter.....	29
13d.	Reactor geometrical model with an outboard tritium breeding blanket, and inboard steel blanket and a bottom limiter.....	29
13e.	Geometrical model for the carbon/copper/water bottom limiter.....	30
13f.	Divertor geometrical model.....	30

LIST OF TABLES

Number		Page
1.	Blanket Parameters for the Nucleonic Analyses.....	5
2.	Impact of the Different Reflector Materials on the Lithium-Lead Blanket Performance.....	5
3.	Recommended Design Parameters for Lithium-Lead and Lithium Blankets.....	23
4.	Design Parameters of Differen Reactor Components.....	25
5.	Blanket Performance Parameters from the Different Geometrical Models with a Full Tritium Breeding Blanket and Without an Impurity Control System.....	31
6.	Impact of the Inboard Blanket Design and the Limiter Options on the Reactor Performance Parameters.....	34
7.	Impact of the Limiter Materials on the Reactor Performance Parameters.....	35
8.	Impact of the Impurity Control Option on the Reactor Performance Parameters.....	36
9.	Benchmark Blanket Parameters.....	38
10.	Atomic Density of the Benchmark Blanket Materials.....	38
11.	Tritium Breeding Results Calculated with Different Methods and Nuclear Data Libraries for Each Benchmark Blanket.....	39
12.	Relative Differences Between the Tritium Breeding Results Calculated with Different Methods and Nuclear Data Libraries for Each Benchmark Blanket.	39

DESIGN ANALYSIS OF SELF-COOLED LIQUID METAL BLANKETS

Y. Gohar

Fusion Power Program
Argonne National Laboratory
Argonne, Illinois 60439

ABSTRACT

A trade-off study of liquid metal self-cooled blankets was carried out to define the performance of these blankets and to determine the potential to operate at the maximum possible values of the performance parameters. The main parameters considered during the course of the study were the tritium breeding ratio (TBR), the blanket energy multiplication factor, the energy fraction lost to the shield, the lithium-6 enrichment in the breeder material, the total blanket thickness, the reflector material selection, and the compositions of the different blanket zones. Also, a study was carried out to assess the impact of different reactor design choices on the reactor performance parameters. The design choices include the impurity control system (limiter or divertor), the material choice for the limiter, the elimination of tritium breeding from the inboard section of tokamak reactors, and the coolant choice for the nonbreeding inboard blanket. In addition, tritium breeding benchmark calculations were performed using different transport codes and nuclear data libraries. The importance of the TBR in the blanket design motivated the benchmark calculations.

I. Introduction

The main blanket functions in a fusion power reactor are to convert the kinetic energy of the deuterium-tritium (DT) neutrons to recoverable heat and produce adequate tritium breeding to supply the tritium fuel requirement during the whole reactor lifetime as well as generate enough surplus tritium to start another reactor within a reasonable period of time. From the reactor design point of view, it is desirable to maximize the recoverable heat produced in the blanket which is defined as the energy deposited in the first wall, breeder, reflector, and plenum per fusion neutron. Another important function of the blanket is to perform as a part of the reactor bulk shield.

In parametric analyses,[1,2] three performance parameters are used to compare the different blanket designs; the tritium breeding ratio (TBR) , the blanket energy multiplication factor, and the energy fraction lost to the shield. The analyses were systematically done to study the changes in these performance parameters due to the following variables: a) the breeder material selection (lithium or lithium-lead), b) the lithium-6 enrichment, c) the breeder zone thickness, d) the reflector material selection, e) the reflector zone thickness, and f) the reflector zone composition. The main results from the parametric analyses are presented in this paper.

Another study was performed to quantify the relative changes in the reactor performance parameters due to the following design choices: a) the impurity control system (limiter or divertor), b) the material choice for the limiter, c) the elimination of the tritium breeding capability from the inboard section of tokamak reactors, and d) the coolant choice for the non-breeding inboard blanket. A self-cooled liquid metal (Li or 17Li-83Pb) blanket was considered with a steel (PCA type) structure. Helium or water was the coolant for the non-breeding blanket. Two limiter blade designs were employed in the analyses.

Accurate prediction of the tritium breeding ratio is an important issue in the blanket design process. Therefore, tritium breeding benchmark calculations were carried out to assess the impact of using different transport codes and nuclear data libraries.

II. Parametric Studies

The neutronic performance of liquid metal (Li or 17Li-83Pb) self-cooled blankets are defined for wide ranges of blanket parameters. Optimum blanket design ranges were obtained for both breeders with steel structure.

II.1 Tritium Breeding

The blanket parameters considered for the study are given in Table I. The first wall and the tritium breeding zone compositions are dictated by thermal hydraulic, structure, and MHD considerations. Different reflector materials (C, Al, Cu, Zr, Mo, W, Pb, H_2O, PCA steel type, and V15Cr5Ti alloy) were employed. The ^6Li enrichment in the 17Li-83Pb changed from natural abundance to 90%. Only natural abundance was considered for the liquid lithium breeder. In general, the blanket does not benefit from lithium-6 enrichment unless a neutron multiplier or a large structural fraction is used in the breeding zone. A shielding zone is included in the calculational model to insure correct boundary conditions at the outer surface of the reflector zone. The one-dimensional discrete ordinates code ANISN[3] was used to perform the transport calculations with a P_3 approximation for the scattering cross sections and an S_8 angular quadrature set. A 67-coupled group nuclear data library (46-neutron and 21-gamma) based on ENDF/B-IV was employed for these calculations. VITAMIN-C[4] and MACKLIB-IV[5] libraries were used to obtain this library.

Lithium and lithium-lead blankets require a reflector zone which has good neutron moderators combined with high Z-materials to absorb the secondary gamma rays. The reflector materials soften the neutron spectrum which increase the $^6Li(n,\alpha)t$ reaction rate. The high Z-reflector materials absorb the secondary gamma rays generated from the blanket and the front section of the shield which causes an increase in the blanket energy multiplication factor. Thus, the use of the reflector zone improves the blanket performance in the following manner: a) it reduces the blanket thickness to achieve a specific tritium breeding ratio, b) it increases the blanket energy multiplication factor, c) it reduces the energy generation in the bulk shield, and d) it reduces the total blanket and shield thickness for a specific blanket performance. The TBR analyses are considered in this section. The other aspects will be discussed in different sections of the report.

A natural lithium-lead blanket, with ferritic steel (HT-9) as a structural material and without a reflector zone, was considered in order to demonstrate the undesirable characteristics of this configuration. For this blanket, a 1.0 m breeder zone thickness is required to achieve a 1.24 TBR. At this thickness, the shield zone absorbs about 0.17 neutrons per fusion neutron and generates about 7% of the total energy. Increasing the breeding zone thickness to 1.2 m reduces the neutron leakage and the energy generation in the shield by a factor of two and increases the TBR from 1.24 to 1.31. Therefore, the 1.2 m breeder zone thickness is required to capture 96% of the total energy generated in the blanket with adequate tritium breeding. Such a thickness has undesirable effects on the reactor design. For a natural liquid lithium breeder, the neutron leakage is greater than the leakage from the corresponding lithium-lead blanket. The neutron leakage from a 1.0 m lithium breeder zone is about 0.5 neutron per fusion neutron which generates problems for the reactor design. Lead is more effective in slowing down the fusion neutrons relative to lithium.

In order to compare and select a reflector material for detail analysis, several materials were used with the same blanket. The blanket has a 50 cm thick lithium-lead zone with a 5 Vol% PCA structural material. The reflector zone is 30 cm thick with a 5 Vol% lithium-lead coolant and another 5 Vol% PCA structure. The ^{6}Li enrichment is 90% to ensure adequate neutron absorption in ^{6}Li for tritium breeding. The other blanket parameters are given in Table 1.

The TBR obtained from this analysis is given in Table 2 as well as the energy generated in the blanket per fusion neutron. The water reflector gives the highest TBR due to the excellent slowing down properties of hydrogen.[6] The carbon reflector produces a 4% lower tritium production relative to water. The high Z-reflector materials produce lower TBRs relative to water or carbon. This is due to more parasitic absorption and less slowing down in the reflector materials. The use of a high pressure water reflector with the self-cooled liquid metal concepts represents an undesirable combination based on safety considerations. The carbon reflector is the choice if a high TBR is the main criterion for the design. The other reflector materials (Cu, Cr, Mo, W, Pb, type PCA steel, and V-15Cr-5Ti alloy) produce about the same TBR as shown in Table 2. Each of these materials has at least one disadvantage from

TABLE 1.

BLANKET PARAMETERS FOR THE NUCLEONIC ANALYSES

Zone Description	Zone Thickness (cm)	Zone Composition (Vol. %)
First Wall	1	50% steel structure 50% liquid metal[a]
Breeder	(BT)[b]	7.5% steel structure 92.5% liquid metal[a]
Reflector	(RT)[b]	C%[b] steel structure D%[b] liquid metal[a] (100-C-D)% reflector material (RM)
Shield	60	90% type Fe1422 steel 10% water

[a] Natural lithium or lithium-lead.
[b] BT, RT, C, and D are variables, where BT is the breeder zone thickness and RT is the reflector zone thickness.

TABLE 2.
IMPACT OF THE DIFFERENT REFLECTOR MATERIALS ON THE LITHIUM-LEAD BLANKET[a] PERFORMANCE

Reflector Material	Tritium Breeding Ratio	Blanket Energy (MeV) Per DT Neutron
Mo	1.54	18.06
Cu	1.55	17.82
W	1.51	17.63
Type PCA Steel	1.59	17.36
H_2O	1.75	17.36
V-15Cr-5Ti Alloy	1.60	17.28
Zr	1.60	17.05
C	1.68	16.96
Pb	1.59	16.48
Al	1.57	16.47

[a]Blanket parameters are listed in Table 1 with the following modifications: 49 cm breeding zone thickness (95% 17Li-83Pb, 5% PCA steel type), 30 cm reflector (5% 17Li-83Pb, 90% reflector, 5% PCA steel type) and 90% ^{6}Li

a reactor design point of view. For example, Cu, Zr, and Mo have long-term radioactive products and lead has a low melting point. The V-15Cr-5Ti alloy and W are expensive materials relative to the others. For these reasons, carbon and steel type reflectors were the choice for more detail analyses.

Carbon and steel with the natural lithium-lead breeder were employed for in-depth analysis. A ferritic steel (HT-9) structure was employed for this analysis. Figures 1 and 2 show the TBR as a function of the reflector zone thickness for different breeding zone thicknesses. The blankets with the steel reflector do not achieve a TBR greater than 0.9 for 90 cm maximum blanket thicknesses (breeder and reflector). The same blanket with a carbon reflector has a TBR greater than 1.2. This performance difference is related to the ratio of the lithium-6 macroscopic absorption cross section, to the total macroscopic absorption cross section in the reflector zone. This ratio is close to unity for the carbon reflector because it is dominated by $^{6}Li(n,\alpha)t$ cross section. For low energy neutrons, the carbon absorption cross section is four to six order of magniudes lower than $^{6}Li(n,\alpha)t$. For the steel reflector, this ratio is less than one because the macroscopic absorption cross section of steel is comparable to lithium-6 which causes a competition between the steel and the lithium on the available neutrons in the reflector zone. This point is clearly demonstrated when the lithium-6 enrichment is increased in the blanket. The TBR increases from 0.9 to 1.5 when the lithium enrichment is 90% instead of the natural enrichment for the same blanket as shown in Figs. 2 and 3.

Based on the above analysis, the natural lithium-lead blanket with carbon reflector can achieve a TBR greater than 1.2. The same blanket with a steel reflector requires a lithium-6 enrichment to obtain a similar TBR. However, the steel reflector produces a higher blanket energy multiplication which is the subject of the next section. Similar behavior is observed with the liquid lithium breeder except both reflectors can achieve a TBR greater than 1.2 with natural lithium.

The higher energy multiplication factor of the liquid metal blankets with steel reflector motivated further in-depth analysis to address the potential of this concept. The results will also apply to other high Z-reflectors (Cu, Mo, and W). The blanket parameters in Table 1 were considered with the lithium-lead breeder where the lithium-6 enrichment (LE) was varied from

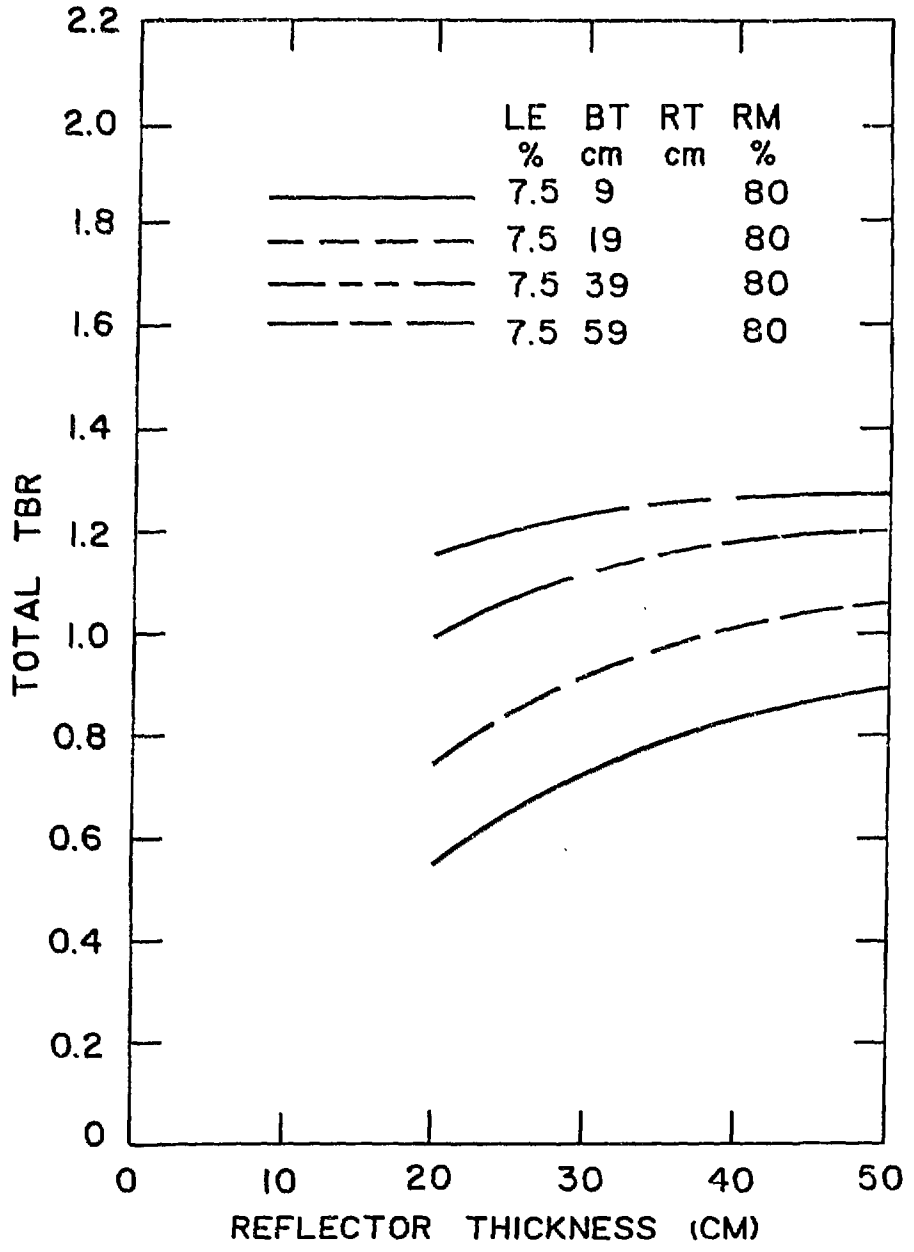

Fig. 1. Tritium breeding ratio as a function of the carbon reflector zone thickness for different lithium-lead breeding zone thicknesses with natural lithium enrichment.

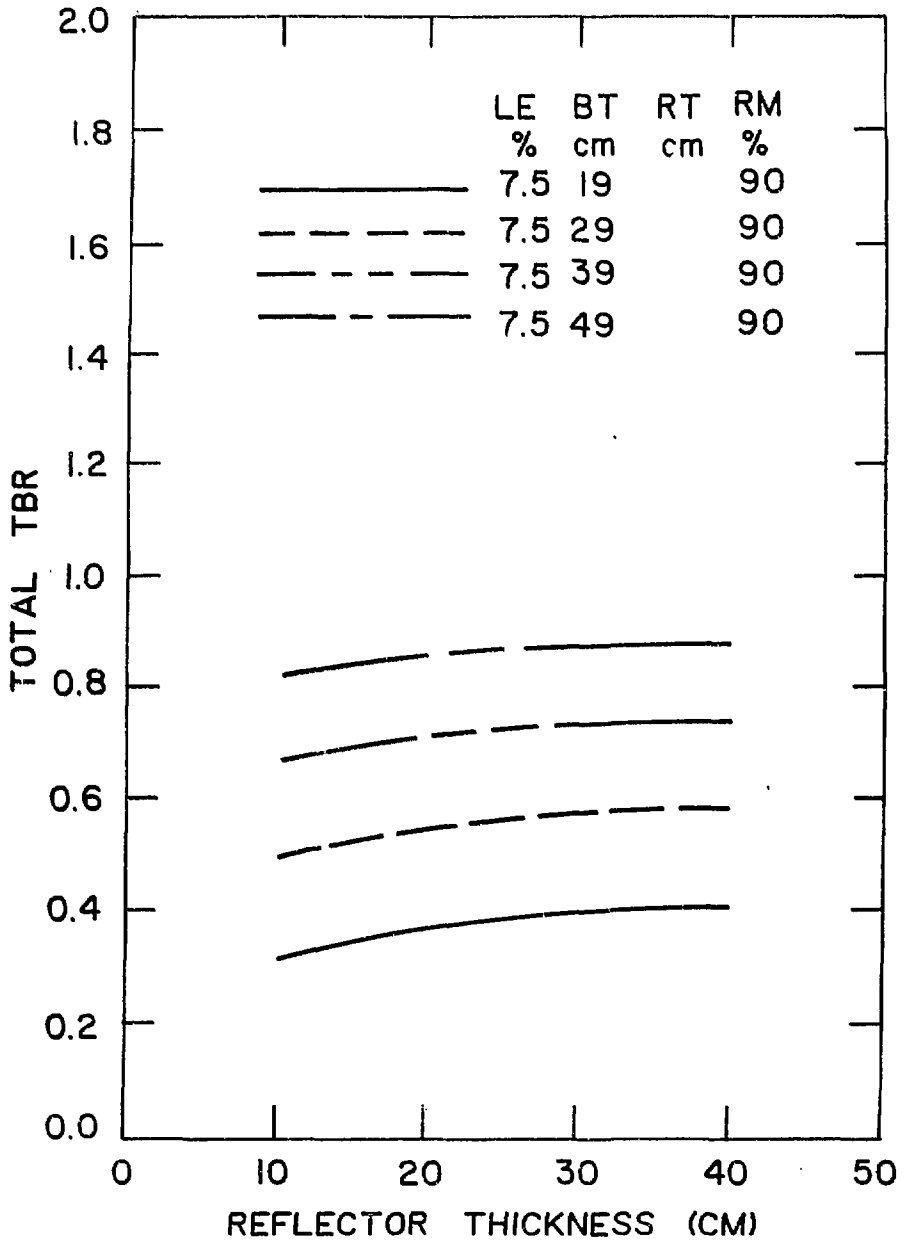

Fig. 2. Tritium breeding ratio as a function of the steel reflector zone thickness for different lithium-lead breeding zone thicknesses with natural lithium enrichment.

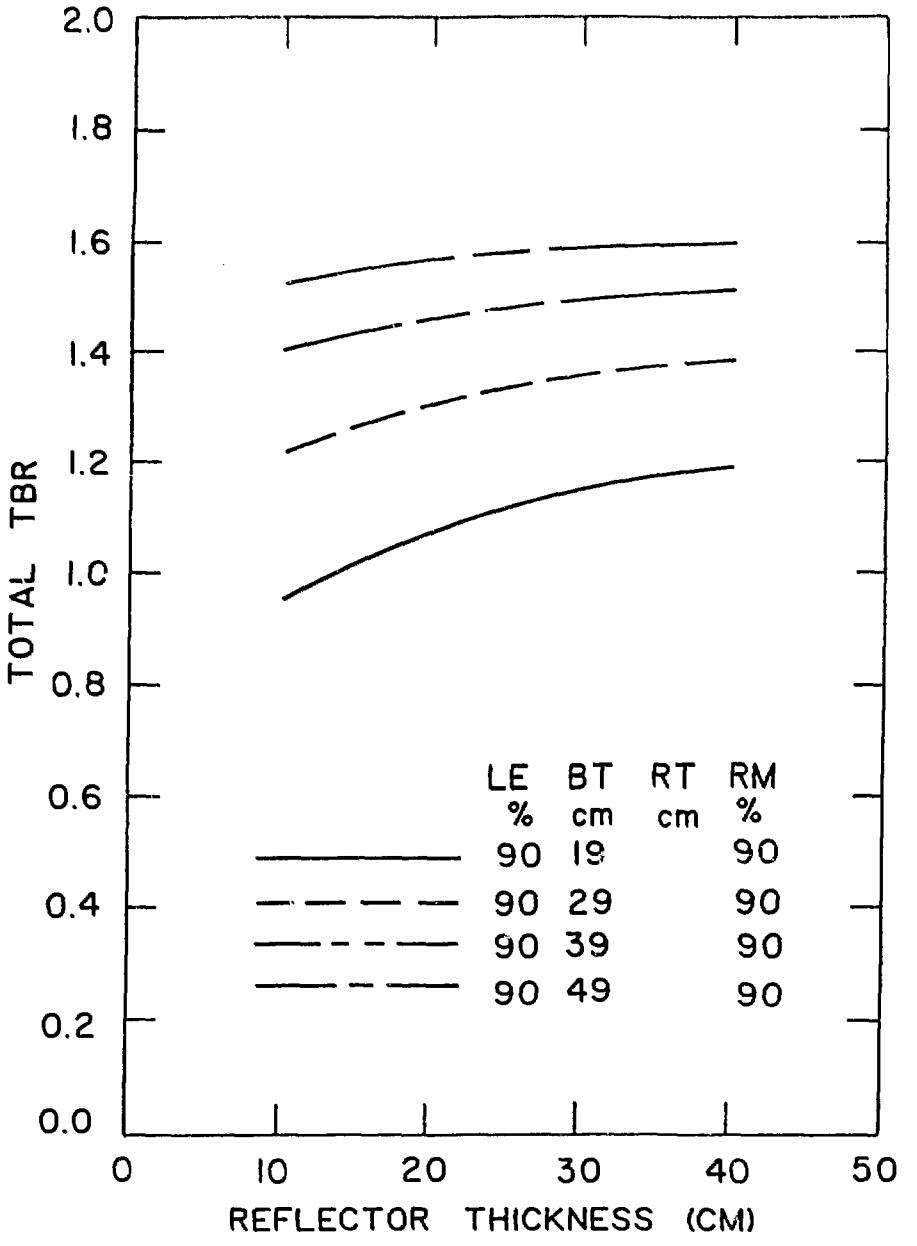

Fig. 3. Tritium breeding ratio as a function of the steel reflector zone thickness for different lithium-lead breeding zone thicknesses with 90% lithium-6 enrichment.

natural enrichment to 90%. The breeder zone thickness (BT) changed from 20 to 50 cm for different reflector zone thicknesses (RT). A sample of the TBR results is shown in Figs. 4 and 5. Other reflector compositions were used in the analysis which show similar trend to the results displayed in Figs. 4 and 5.

With respect to the tritium breeding results, the following observation can be made: a) a TBR up to 1.65 is achievable with a total blanket thickness less than 90 cm, b) the TBR of the natural lithium-lead blanket increases linearly with the breeding zone thickness for any reflector zone thickness up to about 1.2 m total blanket thickness, c) for a specific breeding zone thickness, the TBR ratio increases and reaches a saturation level as the reflector zone thickness increases to about 30 cm, d) at 30% lithium-6 enrichment, a TBR of 1.2 to 1.4 is achievable with a blanket thickness less than one meter, and e) for a specific tritium breeding ratio, the total blanket thickness decreases as the lithium-6 enrichment or the breeding zone thickness increases.

The carbon reflector with the lithium-lead breeder gives similar results to the steel reflector. It requires about 40 cm zone thickness to achieve the TBR saturation value for a specific breeding zone thickness instead of the 30 cm for the steel reflector. Also, the natural lithium blanket with a carbon reflector has a higher tritium breeding potential than the corresponding blanket with a steel reflector.

A similar analysis was performed for the lithium breeder with a steel reflector. Only natural lithium is used because the small steel fraction in the blanket does not require high lithium-6 concentration to achieve the highest possible TBR. Also, the use of natural lithium reduces the breeder material cost. As an example, Fig. 6 shows the TBR as a function of the breeding zone thickness for different reflector zone thicknesses. The results show that a 60 cm lithium blanket produces a TBR greater than 1.2 but it has a low energy multiplication factor. The next section will address this issue in detail. Again, it appears that about a 30 cm steel reflector zone is adequate to achieve the maximum TBR.

II.2 Blanket Energy Multiplication

A main function of the blanket is to produce recoverable heat in suitable conditions for the plant thermal cycle. Thus, a good design strategy is to

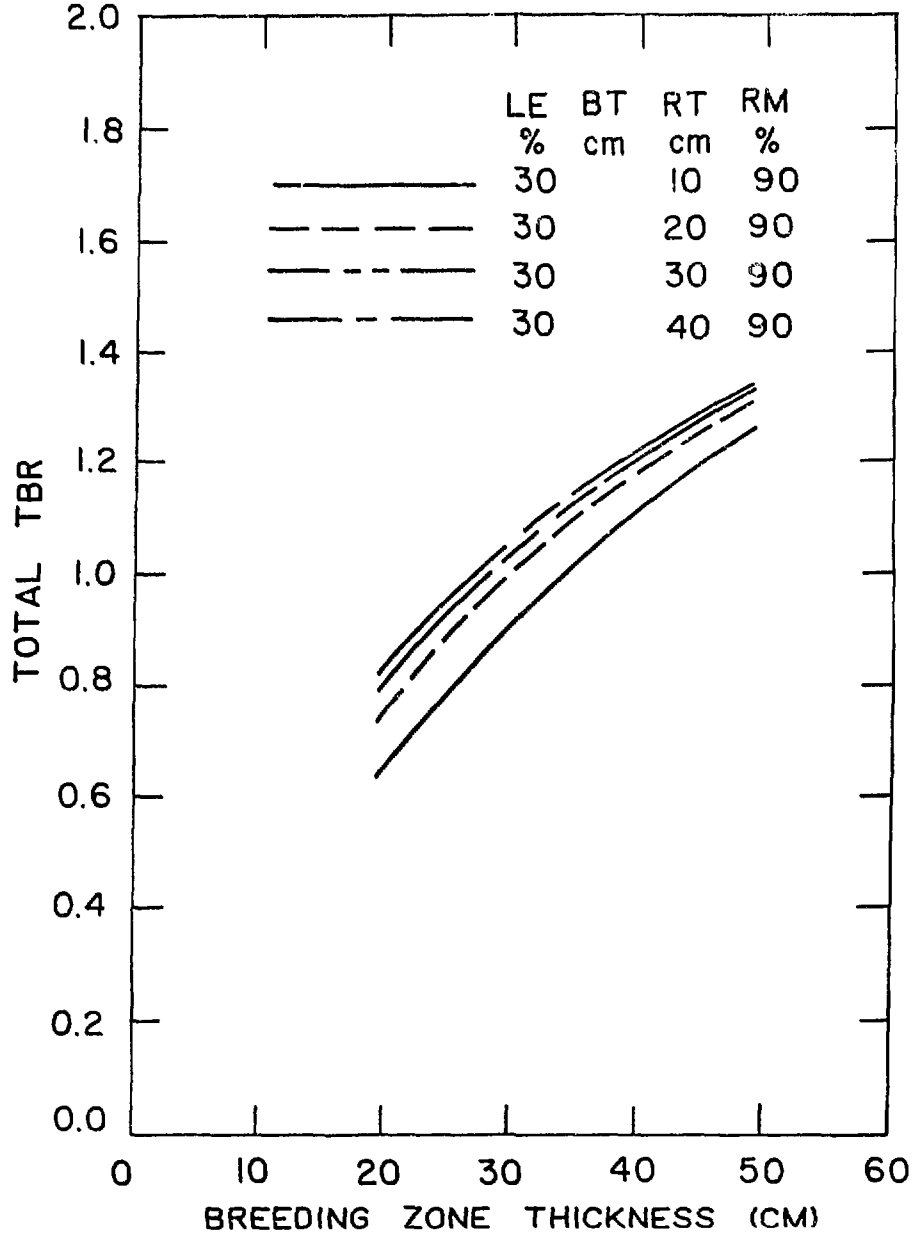

Fig. 4. Tritium breeding ratio as a function of the lithium-lead breeding zone thickness for different steel reflector zone thicknesses with 30% lithium-lead enrichment.

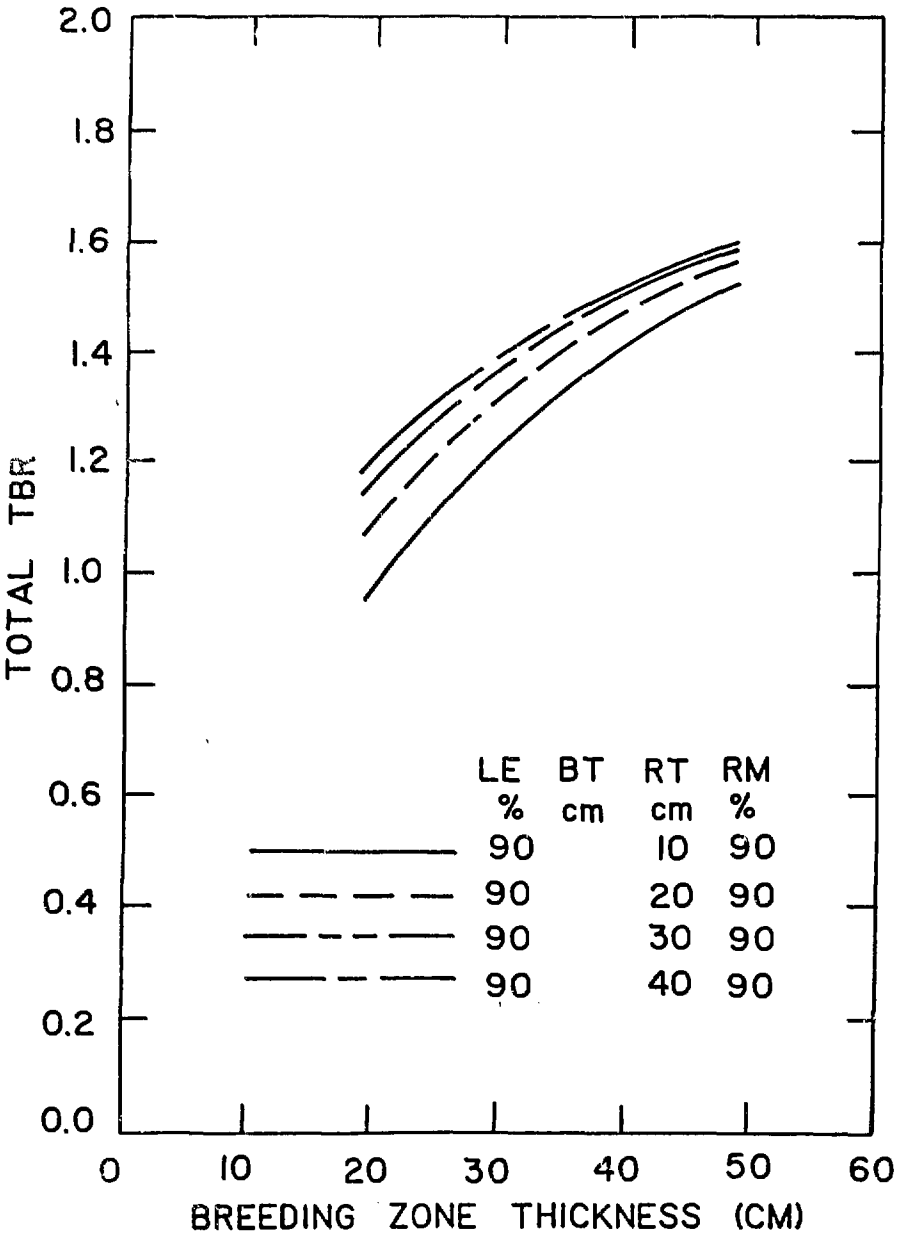

Fig. 5. Tritium breeding ratio as a function of the lithium-lead breeding zone thickness for different steel reflector zone thicknesses with 90% lithium-6 enrichment.

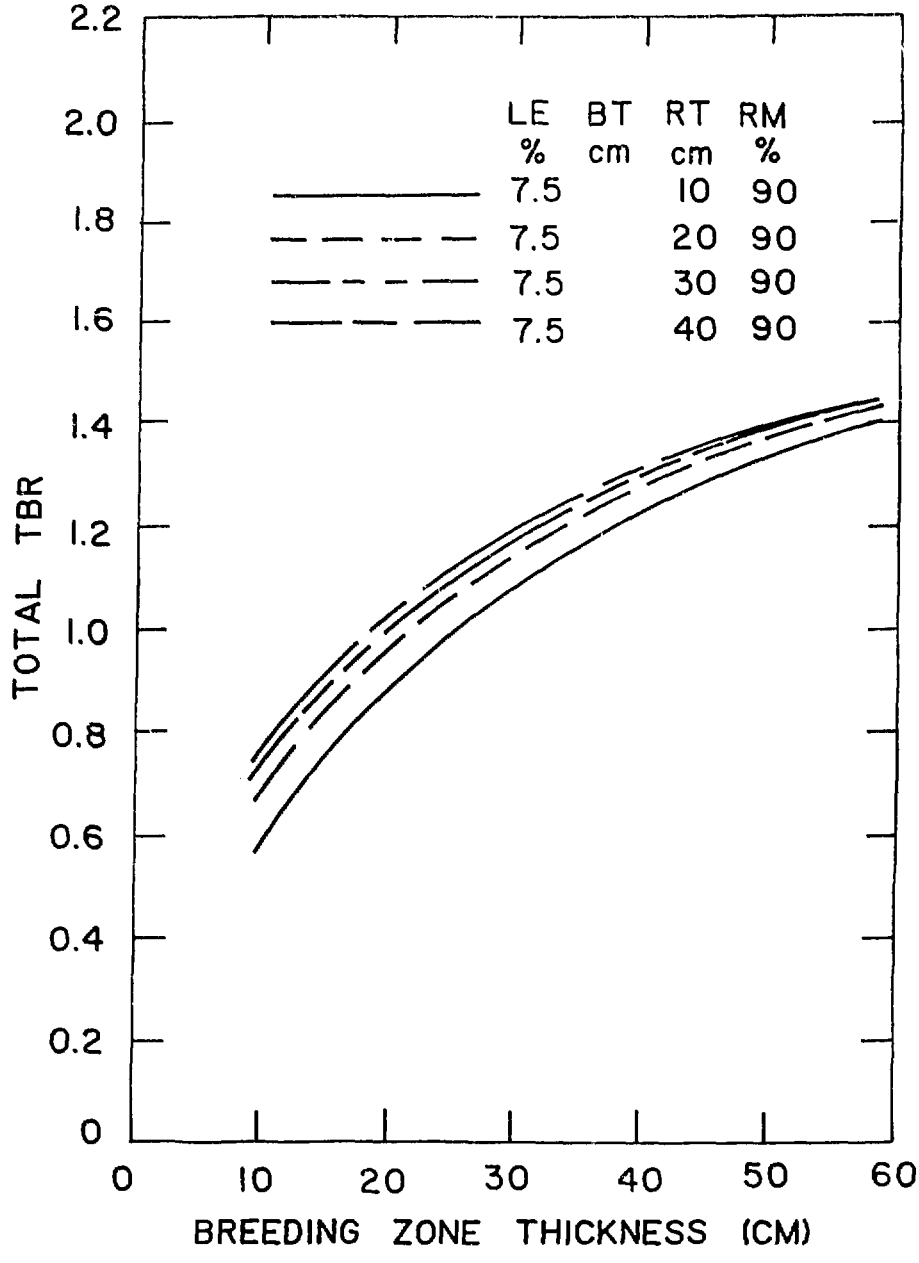

Fig. 6. Tritium breeding ratio as a function of the lithium breeder zone thickness for different steel reflector zone thicknesses with natural lithium enrichment.

maximize the recoverable heat while just meeting the other requirements, such as the required tritium breeding ratio.

Molybdenum, copper, and tungsten reflector materials produce the highest energy deposition in the blanket. Among these three materials, tungsten is the preferred material for two reasons. It has a good shield performance which reduces the total blanket and shield thickness. Also, tungsten does not produce long-term activation and it can be recycled without difficulty. Steel and water reflectors deposit the same amount of energy in the blanket through different mechanism as can be seen from the corresponding TBRs. The blanket with a vanadium reflector produces less energy than the corresponding blanket with steel. The other reflector materials (Zr, C, Pb, and Al) are in a lower rank in terms of the energy deposition per fusion neutron but they produce higher TBRs due to their low absorption cross sections. Again, steel and carbon were used for in-depth analyses for the same reasons discussed in the previous section.

Figures 7 and 8 show the blanket energy multiplication as a function of the lithium-lead breeding zone thickness for different reflector zone thicknesses and two lithium-6 enrichments. The blanket energy multiplication factor decreases as the lithium-6 enrichment increases. As shown before for the lithium-lead breeder in the previous section, the $^{6}Li(n,\alpha)t$ reaction rate increase with the lithium-6 enrichment because more neutrons are absorbed in the lithium-6 with a Q value of 4.8 MeV instead of about 7 to 8 MeV from neutron capture in the steel structure. As a result, a low lithium-6 enrichment should be used to increase the blanket energy multiplication. For both breeder materials, an increase in the reflector zone thickness increases the blanket energy multiplication and the TBR. So, it is always desirable to have the reflector zone thickness in the range of 30 to 40 cm to improve the blanket performance. For blankets with a reflector zone thicknesses less than 30 cm, an increase of the breeding zone thickness improves the blanket energy multiplication factor and the TBR. As the reflector zone thickness exceeds the range of 30 to 40 cm, the blanket energy multiplication slowly decreases with the increase of the breeding zone thickness as shown in Figs. 7 and 8.

Similar results for the carbon reflector with a natural lithium-lead breeder were obtained. For the same blanket, the use of the carbon reflector results in less blanket energy multiplication and higher TBR relative to the

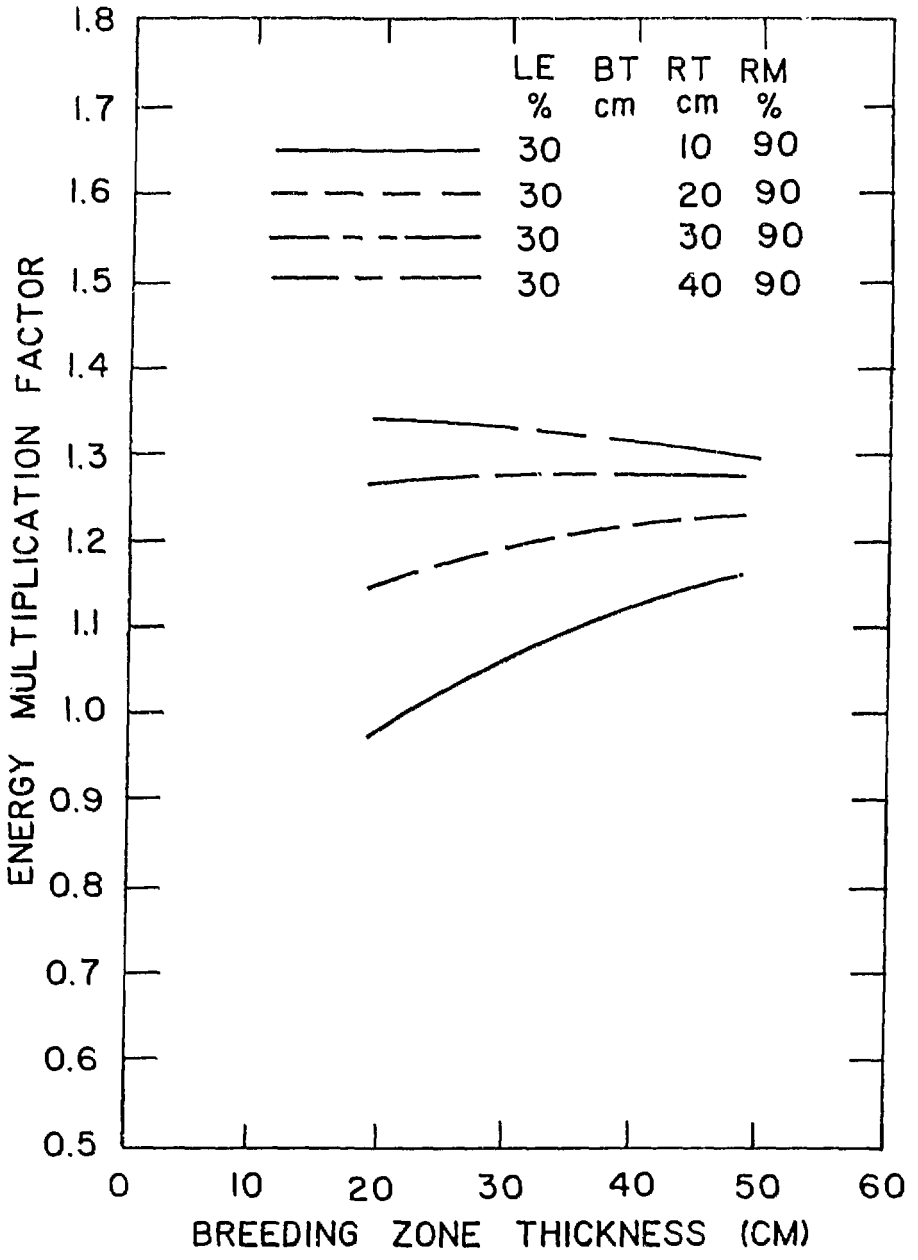

Fig. 7. Blanket energy multiplication factor as a function of the lithium-lead zone thickness for different steel reflector zone thicknesses with 30% lithium-6 enrichment.

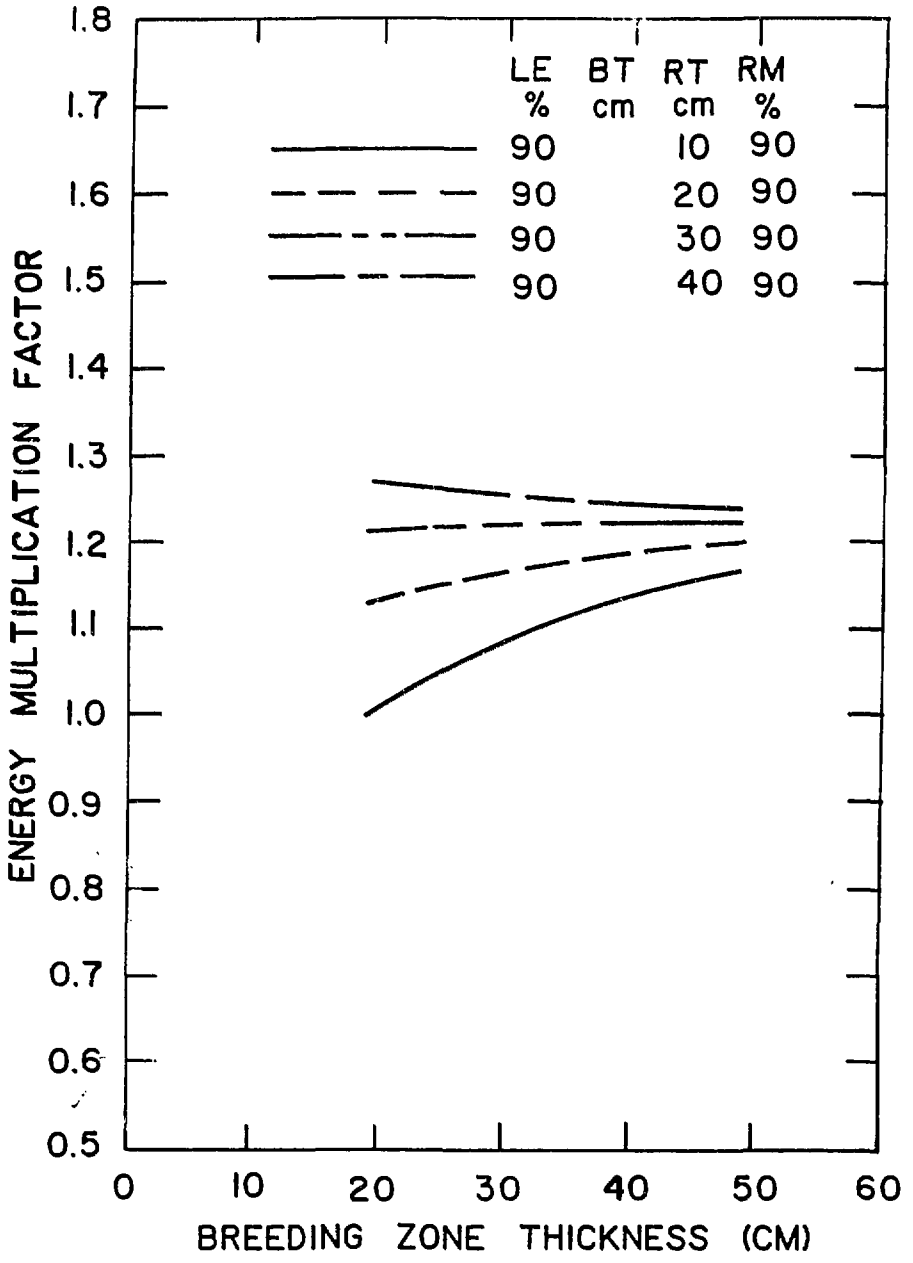

Fig. 8. Blanket energy multiplication factor as a function of the lithium-lead zone thickness for different steel reflector zone thicknesses with 90% lithium-6 enrichment.

steel reflector. The blanket energy multiplication increases to a saturation value as the breeding zone thickness increases for any reflector zone thickness. This observation is different from the steel reflector cases. In fact, the carbon reflector increases the neutron absorption rate in lithium-6 and reduces the neutron leakage from the blanket. This causes an increase in the TBR and the blanket energy multiplication. In the case of the steel reflector, lithium-6 has to compete on the available neutrons with the parasitic absorption in the steel. In this case, the use of a high lithium-6 enrichment increases the TBR but reduces the blanket energy multiplication as explained before.

Figure 9 shows the blanket energy multiplication for the natural liquid lithium breeder as a function of the breeding zone thickness for different reflector zone thicknesses. The results are similar to the lithium-lead breeder with a steel reflector.

II.3 Shield Energy Deposition

The energy generated in the shield system is lost because it is not suitable for power generation. This loss should be minimized to improve the reactor economics by adjusting the blanket dimensions and/or compositions. The plant efficiency drops by about 1% for every 3% of the total energy generated in the shield. Figures 10, 11 and 12 give the energy fraction of the total energy generated in the shield for the same range of the blanket parameters discussed in the previous two sections.

In order to reduce the energy generation in the shield to less than 3% for the blanket with the lithium-lead breeder and the steel reflector, the total blanket thickness should be in the range of 80 to 90 cm thick depending on the lithium-6 enrichment. The corresponding blanket with the natural lithium requires about 90 cm total blanket thickness. The use of 90% lithium-6 enrichment reduces the blanket thickness to about 80 cm. This shows that the use of the 90% lithium-6 enrichment instead of the natural abundance reduces the total blanket thickness only by 10 cm. However, this reduction in thickness is accompanied by more than a 6% reduction in the blanket energy multiplication factor. The corresponding dimensions for the same blanket with the carbon reflector are 60 to 70 cm. These dimensions indicate that the use of carbon reflector results in a 20 cm reduction in the blanket thickness.

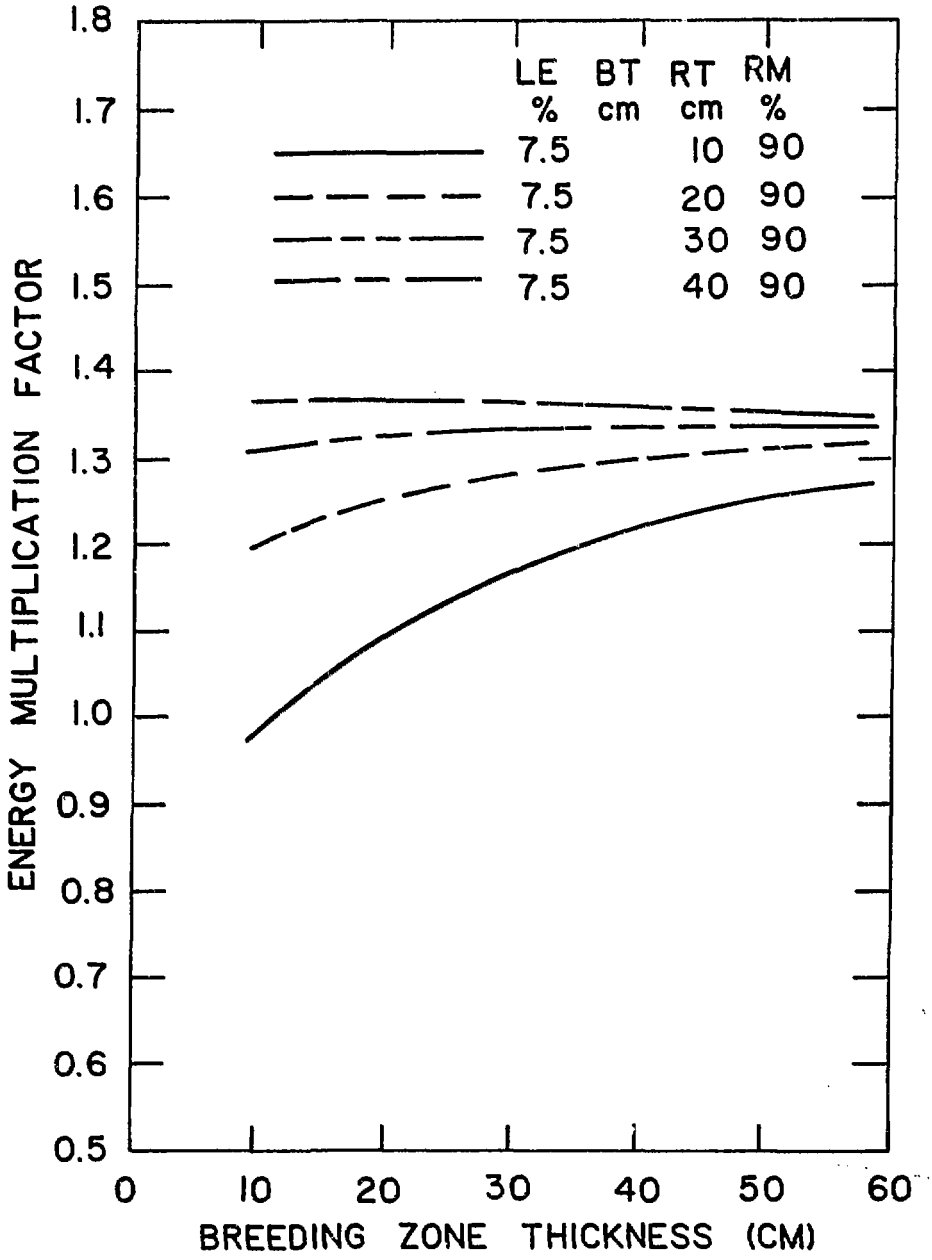

Fig. 9. Blanket energy multiplication factor as a function of the lithium breeder zone thickness for different steel reflector zone thicknesses with natural lithium enrichment (ENDF/B-IV data).

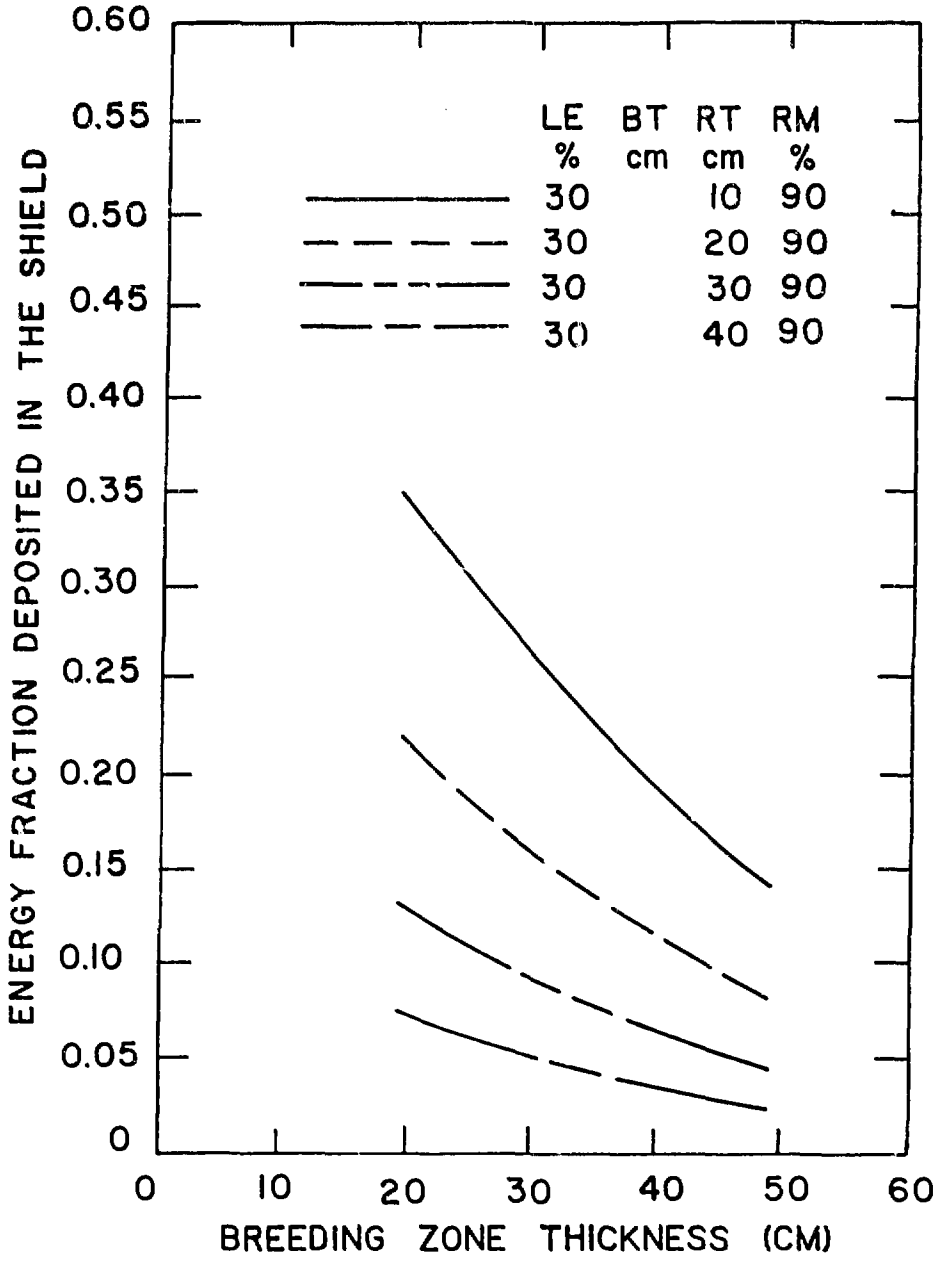

Fig. 10. Fraction of the total energy deposited in the shield as a function of the lithium-lead breeder zone thickness for different steel reflector zone thicknesses with 30% lithium-6 enrichment.

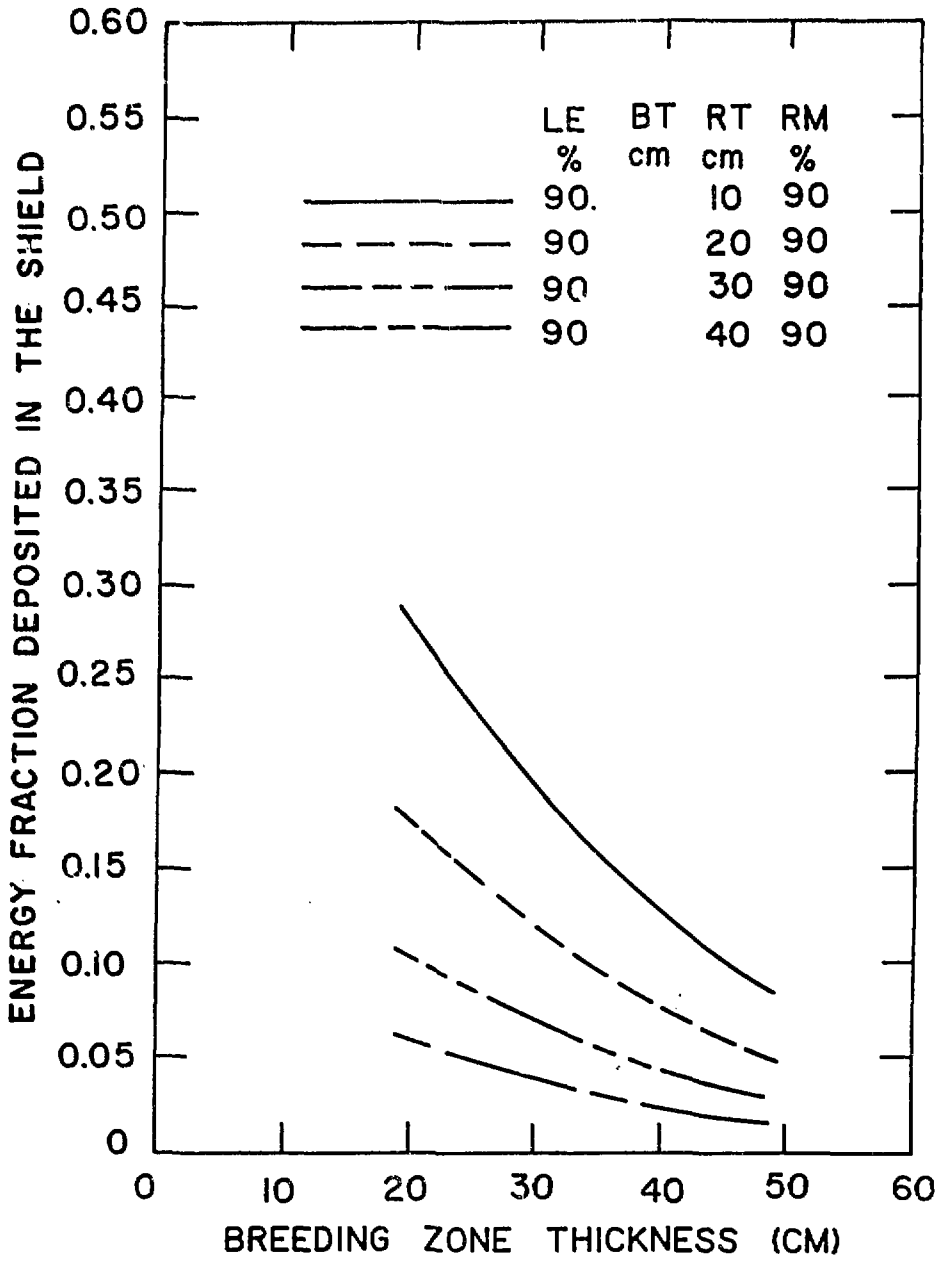

Fig. 11. Fraction of the total energy deposited in the shield as a function of the lithium-lead breeder zone thickness for different steel reflector zone thicknesses with 90% lithium-6 enrichment.

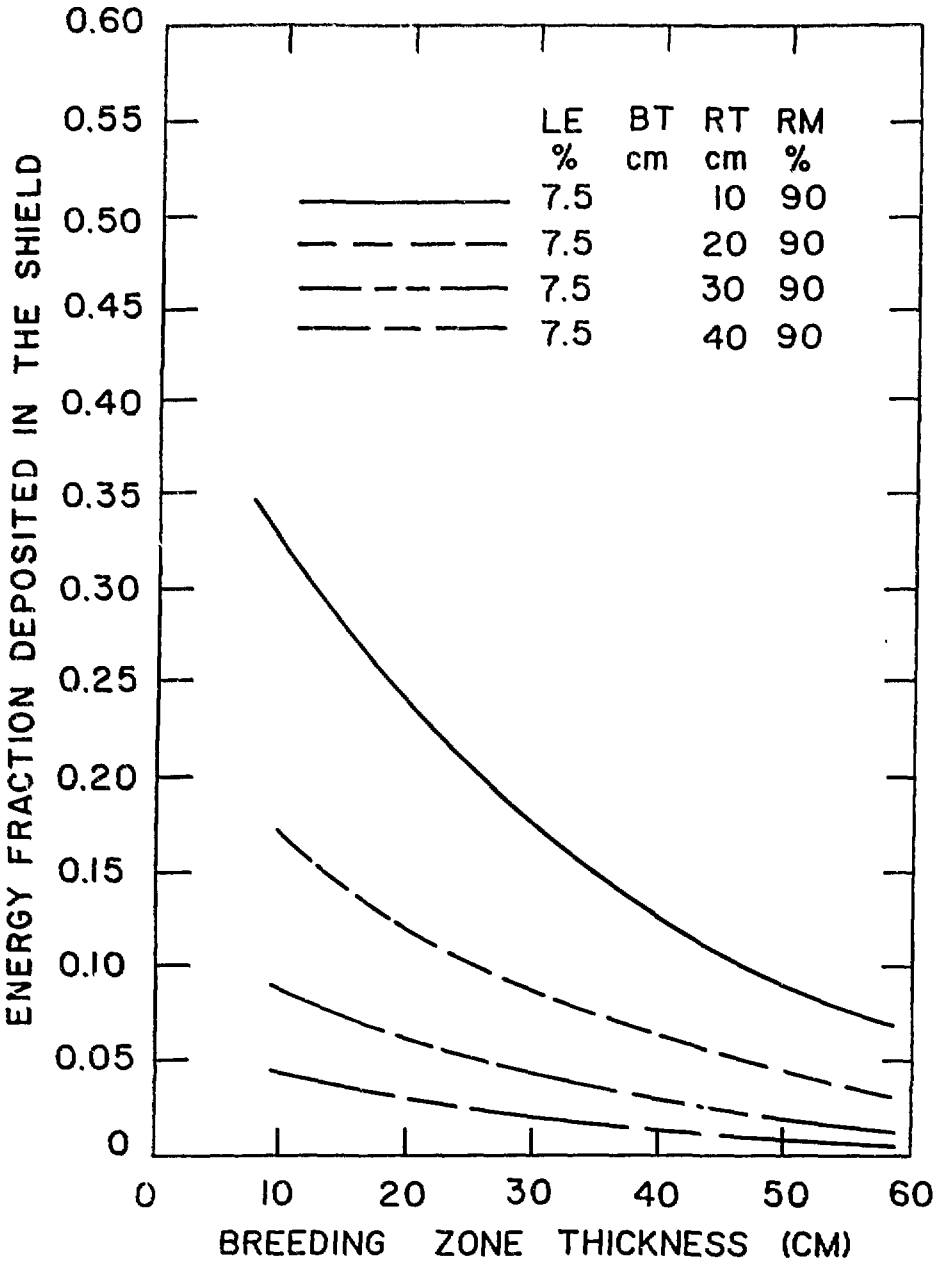

Fig. 12. Fraction of the total energy deposited in the shield as a function of the lithium breeder zone thicknesses for different steel reflector zone thicknesses with natural lithium enrichment.

Again, a blanket with the carbon reflector has a higher TBR and lower blanket energy multiplication than the same blanket with the steel reflector. For the liquid lithium blanket, 60 cm blanket thickness is required. This dimension is equivalent to the lithium-lead blanket with a carbon reflector.

II.4 Optimum Design Parameters for the Liquid Metal Blanket Concepts

From a reactor design point of view, the blanket parameters should be defined to a) satisfy the tritium breeding, thermal hydraulic, and mechanical requirements; b) achieve the highest possible energy multiplication; c) reduce the energy deposition in the shield to less than 3% of the total energy produced; and d) use low cost and natural materials to reduce the reactor capital cost. A 1.2 TBR based on a one-dimensional analysis is used as the basic criterion; the potential for a higher TBR is also considered.

For the lithium-lead blanket concept, the steel reflector produces a higher blanket energy multiplication factor than carbon. The blanket energy multiplication factor shows a continuous decrease as the lithium-6 enrichment increase. Thus, it is desirable to have the lowest possible lithium-6 enrichment subject to achieving adequate tritium breeding. In fact, the 1.2 TBR is achievable with a 30% lithium-6 enrichment as shown in Figs. 4 and 5. Figure 7 shows that the blanket energy multiplication saturates at about 40 cm reflector zone thickness. At this reflector thickness, the energy deposition in the shield is about 3%. This blanket configuration (40 cm breeder and 40 cm reflector) has the potential to achieve a 1.5 TBR if the lithium-6 enrichment is increased to 90% as shown in Fig. 5. Also, a 10 cm increase in the breeding zone thickness changes the TBR from 1.2 to 1.35 for the same lithium-6 enrichment. However, for both cases the blanket energy multiplication decreases as the lithium-6 enrichment or the breeding zone thickness increases. Also, the increase of the lithium-lead concentration in the reflector zone increases the TBR and reduces the blanket energy multiplication factor. Table 3 gives the main parameters for this blanket based on the above analyses.

A similar analysis was performed to define the lithium blanket parameters. Figure 6 shows that a 40 cm breeder zone thickness is required to achieve a 1.2 TBR, a 15% correction factor for $^{7}Li(n;n',\alpha)t$ is included to account for the change in the lithium-7 nuclear data. From a blanket energy

TABLE 3

RECOMMENDED DESIGN PARAMETERS FOR LITHIUM-LEAD AND LITHIUM BLANKETS

Lithium-Lead Blanket	
First Wall Zone (50% 17Li-83Pb, 50% ferritic steel) thickness, cm	1.00
Breeding Zone (92.5% 17Li-83Pb, 7.5% ferritic steel) thickness, cm	39.00
Reflector Zone (20% 17Li-83Pb, 80% ferritic steel) thickness, cm	40.00
Lithium-6 Enrichment, %	30.00
Blanket Energy Multiplication Factor	1.30
Total Energy Multiplication Factor	1.35
Energy Generated in the Blanket Per Fusion Neutron, MeV	18.26
Total Energy Generated in the Reactor Per Fusion Neutron, MeV	19.00
Tritium Breeding Ratio	1.26
Lithium Blanket	
First Wall Zone (50% Li, 50% ferritic steel) thickness, cm	1.00
Breeding Zone (92.5% Li, 7.5% ferritic steel) thickness, cm	39.00
Reflector Zone (10% Li, 90% ferritic steel) thickness, cm	30.00
Lithium-6 Enrichment	Natural
Blanket Energy Multiplication Factor	1.30
Total Energy Multiplication Factor	1.37
Energy Generated in the Blanket Per Fusion Neutron, MeV	18.32
Total Energy Generated in the Reactor Per Fusion Neutron, MeV	19.24
Tritium Breeding Ratio (1.28 Based on ENDF/B-IV)	1.21

multiplication point of view, a reflector zone thickness exceeding 30 cm is required. The energy deposition in the shield is about 3% of the total energy deposition for the 30 cm reflector zone thickness as shown in Fig. 12. The parameters for the lithium blanket is also given in Table 3. The blanket has a potential to achieve a 1.4 TBR by increasing the breeder zone thickness to about 60 cm.

III. Impact of Reactor Design Choices on the Performance Parameters

A study was performed to quantify the impact on the reactor performance parameters of the impurity control system (limiter or divertor), the material choice for the limiter, the elimination of tritium breeding capability from the inboard section of tokamak reactors, and the coolant choice for the non-breeding inboard blanket. A self-cooled liquid metal (lithium and lithium-lead) blankets were considered with a steel (PCA type) structure. Helium or water was the coolant for the non-breeding blanket. Two limiter blade designs were used to assess the sensitivity of the blanket performance. The blanket parameters, the geometrical models, and the results from these studies are presented.

III.1 Computational Models

Two self-cooled liquid metal blankets with different breeder materials were used for this study. The breeder materials are natural liquid lithium and lithium-lead (17Li-83Pb) with a 90% lithium-6 enrichment. The PCA steel alloy is the structure and the reflector material. Table 4 gives the blanket parameters for the inboard and the outboard sections of the reactor. Two limiter blade designs were used in the analysis. The first blade design has a copper structure material, a water coolant, and a carbon tile, which was judged unsatisfactory for liquid metal blanket concepts. The second blade uses the liquid metal coolant of the blanket with a vanadium (V-15Cr-5Ti alloy) structure and a beryllium tile. Table 4 also gives the dimensions and the compositions for the two blades. The divertor design uses only a liquid metal coolant as shown in Table 4.

Several geometrical models were developed for this study based on the STARFIRE design.[9,10] The first geometrical model assumes a tritium breeding blanket for the outboard and the inboard sections of the reactor without an impurity control system as shown in Fig. 13-a. The second geometrical model

TABLE 4

DESIGN PARAMETERS OF DIFFERENT REACTOR COMPONENTS

Component	Parameters (Thickness-Composition[a])
Breeding Blanket	
First wall	1 cm - 50% PCA, 50% liquid metal[b]
Breeder Zone	
Inboard	40 cm - 7.5% PCA, 92.5% liquid metal[b]
Outboard	60 cm - 7.5% PCA, 92.5% liquid metal[b]
Reflector Zone	
Inboard	20 cm - 90% PCA, 10% liquid metal[b]
Outboard	30 cm - 90% PCA, 10% liquid metal[b]
Nonbreeding Blanket	60 cm - 90% PCA, 10% coolant[c]
Shield	
Inboard/Outboard	-- 90% Fe1422 steel alloy, 10% coolant
Water Cooled Limiter	
Coolant	H_2O
Structural material	Copper
Tile material	Carbon
Blade width	72 cm
Blade thickness	4 cm
Duct width	57 cm
Blade composition	1.25 cm[d] - 100% C
	2.50 cm - 50% H_2O, 50% Cu
	0.25 cm - 100% C

TABLE 4 (cont'd)

DESIGN PARAMETERS OF DIFFERENT REACTOR COMPONENTS

Component	Parameters (Thickness-Composition[a])
Liquid Metal Cooled Limiter	
Coolant	Liquid Metal[b]
Structural material	V-15Cr-5Ti alloy
Tile material	Beryllium
Blade width	72 cm
Blade thickness	6 cm
Duct width	57 cm
Blade composition	0.10 cm[d] - 100% Be
	0.15 cm - 100% V-15Cr-5Ti alloy
	0.50 cm - 80% coolant, 20% V-15Cr-5Ti alloy
	1.50 cm - 100% V-15Cr-5Ti alloy
	0.50 cm - 80% coolant, 20% V-15Cr-5Ti alloy
	0.15 cm - 100% V-15Cr-5Ti alloy
	0.20 cm - 100% Be
Divertor	
Coolant	Liquid Metal[b]
Structural material	V-15Cr-5Ti alloy
Tile material	Beryllium
Blade thickness	3.5 cm
Blade composition[a]	1.0 cm[d] -100% beryllium
	2.5 cm - 58% coolant, 42% V-15Cr-5Ti alloy

[a]Volume percent.
[b]Natural lithium or 17Li-83Pb with 90% lithium-6 enrichment.
[c]H_2O or helium.
[d]Surface facing the plasma.

is similar to the first except a non-breeding blanket is used for the inboard section as shown in Fig. 13-b. A bottom limiter was added for both models to study the impact on the reactor performance as shown in Figs. 13-c and 13-d. The details of the limiter geometry are shown in Fig. 13-e. Also, a single null divertor was used instead of the limiter as shown in Fig. 13-f. In addition, two one-dimensional models were developed to compare the one- and three-dimensional results for the cases with a tritium breeding capability for both blanket sections and without an impurity control system.

The three-dimensional Monte-Carlo code MORSE[7] was used to perform the transport calculations with a P_3 approximation for the scattering cross sections, except for the two one-dimensional geometrical models. The one-dimensional discrete ordinates code ANISN[3] was used with P_3S_8 approximations. Again, the 67-coupled group cross-section data library (46 neutron and 21 gamma) used in the parametric studies was employed for the Monte-Carlo calculations.

III.2 Tritium Breeding and Energy Deposition Changes

The reactor geometrical models without an impurity control system and with a tritium breeding capability in the inboard section were used to calculate the blanket performance parameters. The results from the ANISN calculations show that the poloidal and the toroidal geometrical models predict very closely the TBR and the blanket energy deposition (BED) values as shown in Table 5. However, the poloidal model does not account for the smaller inboard blanket thickness which causes a small increase in the TBR and decrease in the BED of about 1% in both parameters. This is due to the increase in the neutron absorption rate in the steel shield which deposits more energy relative to the neutron capture in the lithium-6, as mentioned before. The main difference in the results from both models is in the prediction of the shield energy deposition (SED) as shown in Table 5. For the reactor under consideration, the poloidal model underestimates the SED by a factor of two relative to the toroidal model (the expected value). A MORSE calculation for the first geometrical model shown in Fig. 13-a was performed to compare with the one-dimensional calculations. The results given in Table 5 show that the MORSE results are in good agreement with the one-dimensional toroidal results calculated by ANISN. For example, the relative difference in the TBR is about 0.7% which is less than the statistical error in the Monte-Carlo calculations.

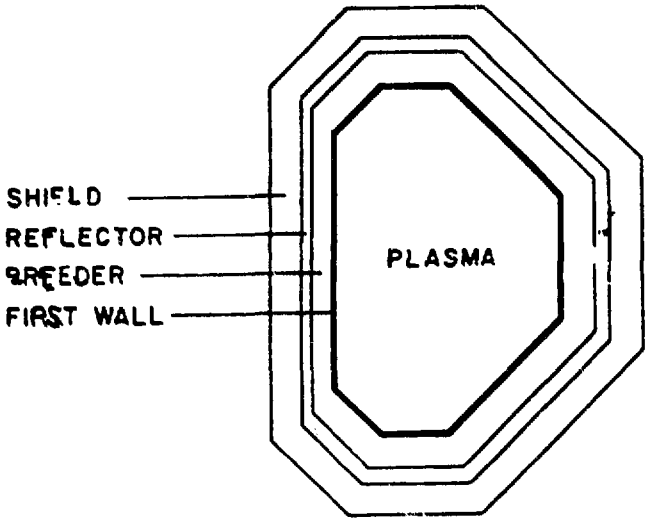

Fig. 13a. Reactor geometrical model with a tritium breeding blanket for both inboard and outboard sections.

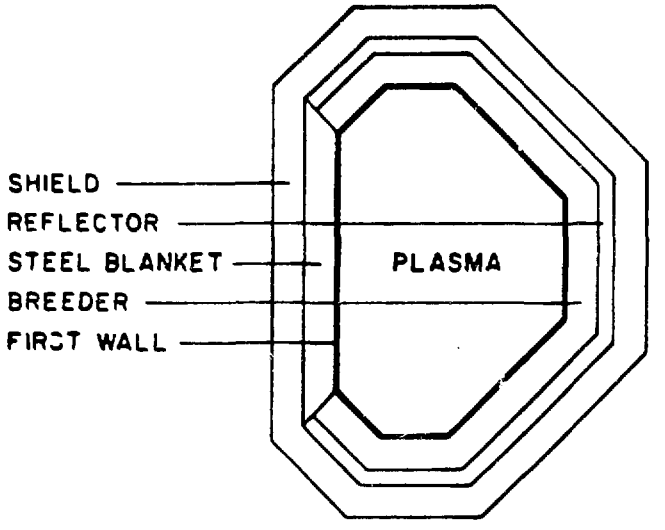

Fig. 13b. Reactor geometrical model with an outboard tritium breeding blanket and an outboard steel blanket.

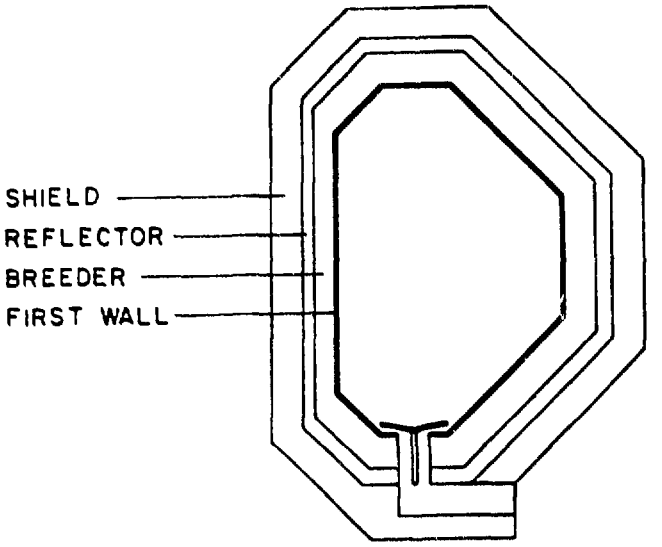

Fig. 13c. Reactor geometrical model with a tritium breeding blanket for both the inboard and outboard sections with a bottom limiter.

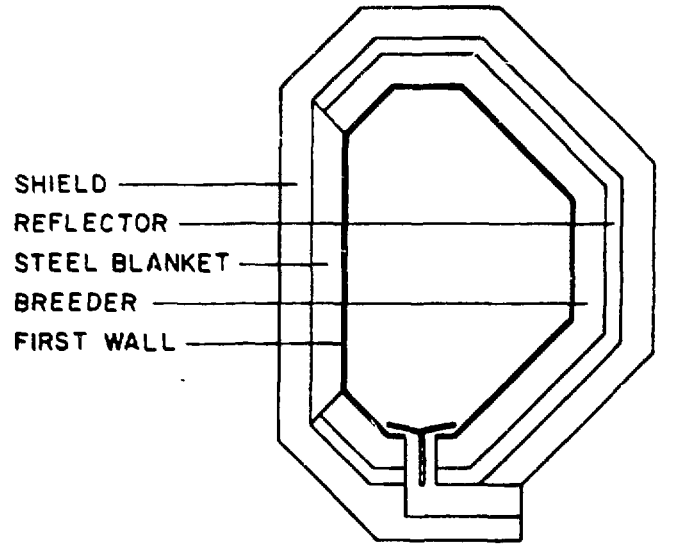

Fig. 13d. Reactor geometrical model with an outboard tritium breeding blanket, an inboard steel blanket and a bottom limiter.

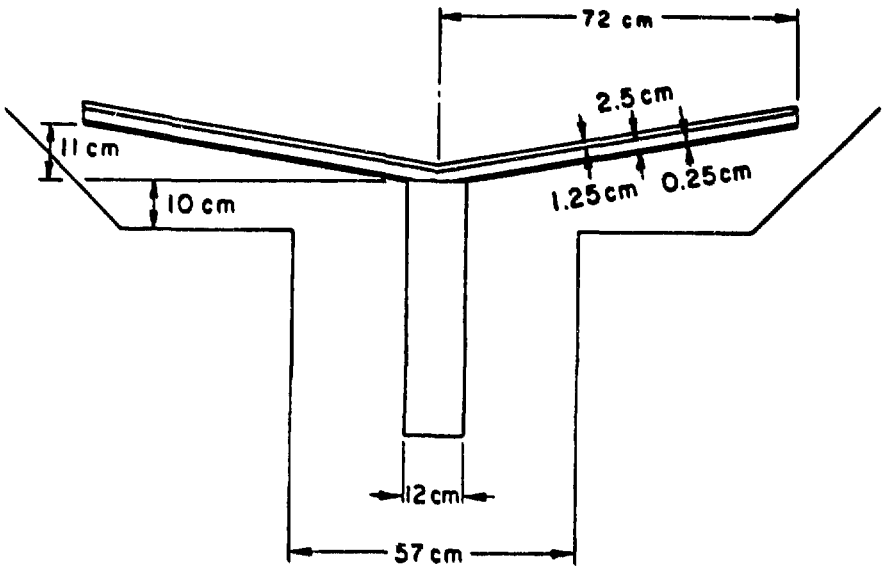

Fig. 13e. Geometrical model for the carbon/copper/water bottom limiter.

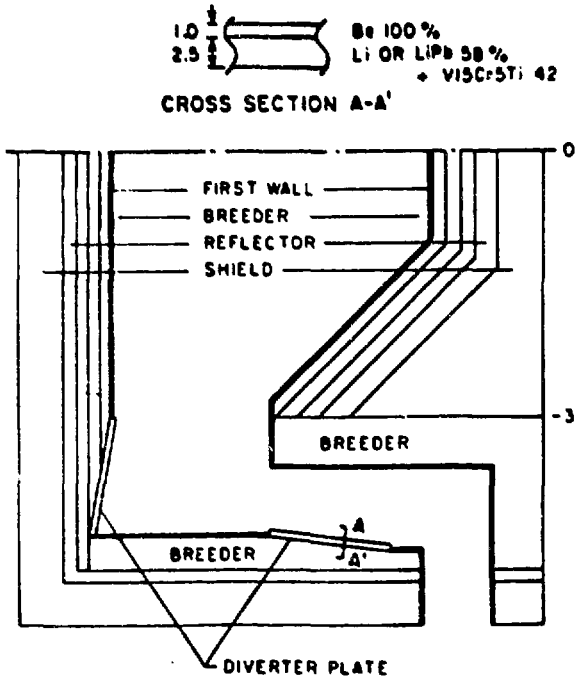

Fig. 13f. Divertor geometrical model.

TABLE 5
BLANKET PERFORMANCE PARAMETERS FROM THE DIFFERENT GEOMETRICAL MODELS WITH A FULL TRITIUM BREEDING BLANKET AND WITHOUT AN IMPURITY CONTROL SYSTEM

Lithium Breeder

Geometrical model	1-D poloidal	1-D toroidal	3-D
Transport code	ANISN	ANISN	MORSE
$^{6}Li(n,\alpha)T$ reaction rate per DTn	0.906	0.909	0.880
$^{7}Li(n,n'\alpha)T$ reaction rate per DTn[a]	0.470	0.463	0.479
Tritium breeding ratio[a]	1.376	1.372	1.359
Blanket energy deposition, MeV/DTn	18.79	18.95	18.78
Shield energy deposition, MeV/DTn	0.28	0.44	0.40

Lithium-Lead Breeder

Geometrical model	1-D poloidal	1-D toroidal	3-D
Transport code	ANISN	ANISN	MORSE
$^{6}Li(n,\alpha)T$ reaction rate per DTn	1.648	1.632	1.606
$^{7}Li(n,n'\alpha)T$ reaction rate per DTn[a]	0.003	0.003	0.003
Tritium breeding ratio[a]	1.651	1.635	1.609
Blanket energy deposition, MeV/DTn	17.48	17.67	17.07
Shield energy deposition, MeV/DTn	0.20	0.39	0.30

[a]The $^{7}Li(n,n'\alpha)T$ reaction rates are reduced by 15% to account for the change in the ^{7}Li cross sections.

In all of the Monte Carlo calculations, the fractional standard deviations are less than 1.5% and 3% for the TBR and the energy deposition, respectively.

Several MORSE calculations were performed to study the change in the TBR and the energy deposition due to different design options selected for the inboard blanket and impurity control system. The results in Table 6 address the impact of the copper limiter (carbon tile, copper structure, and water coolant) and the different inboard blanket options on the TBR and the energy deposition for the lithium and the lithium-lead blankets. These results show that the use of the copper limiter reduces the TBR by about 4% and 5% for the lithium and the lithium-lead blankets, respectively. This conclusion is consistent with the previous analysis for a Li_2O blanket performed for FED/INTOR.[11] Also, the BED is reduced and the SED is increased significantly as shown in Table 6.

For both blankets, the inboard blanket was changed and the reactor performance parameters are calculated as shown in Table 6. The PCA/H_2O inboard blanket with the copper limiter produces the largest impact on the TBR, the losses are 17% and 24% for the lithium and the lithium-lead blanket concepts, respectively, relative to the full breeding case without the limiter. Comparing both liquid blankets, the lithium-lead blanket has a softer neutron spectrum which makes this blanket concept sensitive to changes in the plasma chamber. For the PCA/H_2O inboard blanket with the lithium-lead outboard blanket the loss in the TBR is proportional to the loss in the surface area available for the tritium breeding. The BED is increased by about 6% which results from the exothermic absorption of the low energy neutrons in the steel structure and less leakage to the shield. The corresponding impact for the helium coolant instead of water in the inboard blanket is less because the neutron spectrum is harder. For example, the TBR of the He cooled inboard blanket is 1.30 compared to 1.23 for water coolant. Also, the helium coolant generates 3% less energy in the blanket and 40% more energy in the shield relative to the water coolant.

The same observations about the impact of the inboard blanket coolant are valid for the lithium blanket. However, the BED decreases when the limiter and non-breeding blanket are employed for the impurity control system and the inboard section, respectively. This is the contrary to the results of the

lithium-lead blanket concept. The increase in neutron streaming through the limiter duct is causing this loss in the BED because of the harder neutron spectrum. The PCA/H_2O inboard blanket increases the BED by 0.5 MeV per DTn and reduces SED by 30% relative to the lithium inboard blanket because of the neutron slowing down process.

The effect of the limiter design is analyzed for both blankets as shown in Table 7. For the lithium blanket, the use of the vanadium limiter (beryllium tile, V-15Cr-5Ti structure, lithium coolant) acts as a neutron multiplier region which cause an increase in the TBR and the BED. In addition, the vanadium alloy has a low neutron capture cross section relative to the copper which also improves the neutron economy. For the lithium-lead blanket, the effect of the limiter on the blanket performance is different because it is a thermal blanket. The low absorption cross section of the vanadium structure relative to the copper causes an increase in the TBR. However, from the energy multiplication point of view, copper produces a higher BED as shown in Table 7.

The limiter and the divertor impurity control options with vanadium structure were considered to compare their effect on the reactor performance parameters. Table 8 gives the performance parameters for each impurity control option with different inboard blankets for both liquid blankets. The results show that the divertor option has a small advantage over the limiter. The TBR is about the same for both options. However, the BED is higher with the divertor because the neutron absorption rate in the vanadium structure is lower. This means more neutrons are absorbed in the steel structure which results in more energy due to the difference in the Q values of both materials. The reactor with a divertor produces about 4% more energy than the limiter case.

IV. Tritium Breeding Benchmark Calculations for Liquid Lithium Blankets

Tritium breeding benchmark calculations were performed by using different transport codes and data libraries. ANISN[3] and MCNP[12] transport codes were employed. ANISN is a one-dimensional, multi-group, neutron/photon transport code using the discrete ordinates method and the Legendre expansion approximation for the scattering cross sections. MCNP is a three-dimensional, continuous energy, neutron/photon transport code using the Monte Carlo method. Four nuclear data libraries based on ENDF/B version IV and V were

TABLE 6
IMPACT OF THE INBOARD BLANKET DESIGNS AND THE LIMITER OPTIONS
ON THE REACTOR PERFORMANCE PARAMETERS

Lithium Breeder				
Inboard blanket materials	Li/PCA	Li/PCA	PCA/H_2O	PCA/He
Computational model	3-D/MORSE	3-D/MORSE	3-D/MORSE	3-D/MORSE
Impurity control option	None	Cu-limiter	Cu-limiter	Cu-limiter
$^6Li(n,\alpha)T$ reaction rate per DTn	0.880	0.852	0.739	0.781
$^7Li(n,n'\alpha)T$ reaction rate per DTn[a]	0.479	0.453	0.389	0.389
Tritium breeding ratio[a]	1.359	1.305	1.128	1.170
Blanket energy deposition, MeV/DTn	18.78	18.02	18.53	18.26
Shield energy deposition, MeV/DTn	0.40	0.51	0.35	0.46
Lithium-Lead Breeder				
Inboard blanket materials	17Li-83Pb/ PCA	17Li-83Pb/ PCA	PCA/H_2O	PCA/He
Computational model	3-D/MORSE	3-D/MORSE	3-D/MORSE	3-D/MORSE
Impurity control option	None	Cu limiter	Cu limiter	Cu limiter
$^6Li(n,\alpha)T$ reaction rate per DTn	1.606	1.522	1.228	1.294
$^7Li(n,n'\alpha)T$ reaction rate per DTn[a]	0.003	0.003	0.002	0.002
Tritium breeding ratio[a]	1.609	1.525	1.230	1.296
Blanket energy deposition, MeV/DTn	17.07	16.65	17.71	17.26
Shield energy deposition, MeV/DTn	0.30	0.43	0.29	0.41

[a]The ^7Li $(n,n'\alpha)T$ reaction rates are reduced by 15% to account for the change in the ^7Li cross sections.

TABLE 7
IMPACT OF THE LIMITER MATERIALS ON THE REACTOR PERFORMANCE PARAMETERS

Lithium Breeder				
Inboard blanket materials	Li/PCA	PCA/He	Li/PCA	PCA/He
Computational model	3-D/MORSE	3-D/MORSE	3-D/MORSE	3-D/MORSE
Limiter structural material	Copper	Copper	V15Cr5Ti	V15Cr5Ti
$^{6}Li(n,\alpha)T$ reaction rate per DTn	0.852	0.781	0.891	0.805
$^{7}Li(n,n'\alpha)$ reaction rate per DTn[a]	0.453	0.389	0.456	0.397
Tritium breeding ratio[a]	1.305	1.170	1.347	1.202
Blanket energy deposition, MeV/DTn	18.02	18.26	18.23	18.34
Shield energy deposition, MeV/DTn	0.51	0.46	0.49	0.39
Lithium-Lead Breeder				
Inboard blanket materials	17Li-83Pb/PCA	PCA/He	17Li-83Pb/PCA	PCA/He
Computational model	3-D/MORSE	3-D/MORSE	3-D/MORSE	3-D/MORSE
Limiter structural material	Copper	Copper	V15Cr5Ti	V15Cr5Ti
$^{6}Li(n,\alpha)T$ reaction rate per DTn	1.522	1.296	1.551	1.334
$^{7}Li(n,n'\alpha)T$ reaction rate per DTn[a]	0.003	0.002	0.003	0.002
Tritium breeding ratio[a]	1.525	1.298	1.554	1.336
Blanket energy deposition, MeV/DTn	16.65	17.26	16.53	17.07
Shield energy deposition, MeV/DTn	0.43	0.41	0.41	0.38

[a]The $^{7}Li(n,n'\alpha)T$ reaction rates are reduced by 15% to account for the change in the ^{7}Li cross sections.

TABLE 8
IMPACT OF THE IMPURITY CONTROL OPTION ON THE REACTOR PERFORMANCE PARAMETERS

Lithium Breeder				
Inboard blanket materials	Li/PCA	PCA/He	Li/PCA	PCA/He
Computational model	3-D/MORSE	3-D/MORSE	3-D/MORSE	3-D/MORSE
Impurity control option	Divertor	Divertor	Limiter	Limiter
Divertor or limiter structural material	V15Cr5Ti	V15Cr5Ti	V15Cr5Ti	V15Cr5Ti
$^{6}Li(n,\alpha)T$ reaction rate per DTn	0.877	0.776	0.891	0.805
$^{7}Li(n,n'\alpha)T$ reaction rate per DTn[a]	0.473	0.401	0.456	0.397
Tritium breeding ratio[a]	1.350	1.177	1.347	1.202
Blanket energy deposition, MeV/DTn	18.56	18.93	18.23	18.34
Shield energy deposition, MeV/DTn	0.49	0.34	0.49	0.39
Lithium-Lead Breeder				
Inboard blanket materials	17Li-83Pb/ PCA	PCA/He	1Li-83Pb/ PCA	PCA/He
Computational model	3-D/MORSE	3-D/MORSE	3-D/MORSE	3-D/MORSE
Impurity control option	Divertor	Divertor	Limiter	Limiter
Divertor or limiter structural material	V15Cr5Ti	V15Cr5Ti	V15Cr5Ti	V15Cr5Ti
$^{6}Li(n,\alpha)T$ reaction rate per DTn	1.581	1.317	1.551	1.334
$^{7}Li(n,n'\alpha)T$ reaction rate per DTn[a]	0.002	0.003	0.003	0.002
Tritium breeding ratio[a]	1.583	1.320	1.554	1.336
Blanket energy deposition, MeV/DTn	17.13	17.80	16.53	17.07
Shield energy deposition, MeV/DTn	0.38	0.36	0.41	0.38

[a]The $^{7}Li(n,n'\alpha)T$ reaction rates are reduced by 15% to account for the change in the ^{7}Li cross sections.

used in the calculations. Vitamin-C[4] and MACKLIB-IV[5] libraries were collapsed to a 46-neutron groups structure for ENDF/B-IV ANISN calculations. Also, the Vitamin-E[13] library was collapsed to the same group structure for the ENDF/B-V ANISN calculations. MCNP employed two continuous energy libraries based on the ENDF/B version IV and V.

A natural liquid lithium blanket with PCA as a structural and reflector material was used for the benchmark. The blanket parameter is given in Table 9 as well as the number of intervals for the discrete coordinate calculations. The ANISN calculations were performed with an S_8 symmetrical angular quadrature set and a P_3 approximation for the scattering cross sections. The neutron source distribution is uniform in the plasma volume and the energy range of the first neutron group (13.499 to 14.918 MeV) for all the calculations. The atomic density of each blanket material is given in Table 10. The fractional standard deviation in the MCNP results is less than 1.5% for all these calculations.

The breeding zone thickness was varied from 39 to 79 cm with a 20 cm step. The TBR was calculated for each blanket four times using the different combinations of the transport codes and the data libraries. Table 11 gives the TBR results for the three blankets. The relative differences between the TBR results for each liquid lithium blanket are given in Table 12. For the same data base (ENDF/B-IV or V), the TBRs calculated by MCNP or ANISN have a good agreement as shown in Table 11. The differences between MCNP and ANISN results have a maximum value of 1.33%. This maximum difference is less than the 1.5% statistical error in the MCNP results.

However, the difference between ENDF/B version IV and V is about 4.6 to 5.6% which is mainly related to the correction in the lithium-7 cross section. These results lead one to conclude that the uncertainty in the TBR for this liquid lithium blanket concept is about 1% due to nuclear data processing, multigroup treatment, and numerical errors from the transport codes. Also, a similar conclusion was found for the lithium-lead blanket with a total thickness less than 80 cm[14].

V. Conclusions

The results of the parametric study are as follows: a) the lithium-lead blanket achieves a higher TBR with a smaller blanket thickness relative to the

TABLE 9
BENCHMARK BLANKET PARAMETERS

Zone Description	Radius cm From	To	No. of Intervals Per Zone	Composition Vol. %
Plasma	0	130	5	Vacuum
Scrape-off	130	150	1	Vacuum
First Wall	150	151	1	50% PCA, 50% Li
Breeding	151	190	39	7.5% PCA, 92.5% Li
Reflector	190	210	20	90% PCA, 10% Li
Shielding	210	270	50	90% Fe1422, 10% H_2O

TABLE 10
ATOMIC DENSITY OF THE BENCHMARK BLANKET MATERIALS

Material	Element	Atomic Density, Atom/b-cm
H_2O	H	6.700-2
	O	3.350-2
Li	^6Li	3.450-3
	^7Li	4.255-2
PCA Steel	Cr	1.274-2
	Ni	1.290-2
	Fe	5.499-2
	C	1.971-4
Fe1422 Alloy	C	2.309-3
	Cr	1.843-3
	Mn	1.219-2
	Fe	6.953-2
	Ni	1.580-3

TABLE 11
TRITIUM BREEDING RESULTS CALCULATED WITH DIFFERENT METHODS AND NUCLEAR DATA LIBRARIES FOR EACH BENCHMARK BLANKET

Data Base	Transport Code	Blanket Thickness, cm (First Wall & Breeding Zone Thickness/ Reflector Zone Thickness) 40/20	60/20	80/20
ENDF/B-IV	ANISN	1.2832	1.4471	1.5333
ENDF/B-IV	MCNP	1.2695	1.4338	1.5288
ENDF/B-V	ANISN	1.2103	1.3735	1.4626
ENDF/B-V	MCNP	1.1984	1.3656	1.4434

TABLE 12.
RELATIVE DIFFERENCES BETWEEN THE TRITIUM BREEDING RATIOS CALCULATED WITH DIFFERENT METHODS AND NUCLEAR DATA LIBRARIES FOR EACH BENCHMARK BLANKET

	Blanket Thickness, cm (First Wall & Breeding Zone Thicknesses Reflector Zone Thickness) 40/20	60/20	80/20
(ANISN - MCNP) × 100/MCNP with ENDF/B-IV	1.08	0.93	0.29
(ANISN - MCNP) × 100/MCNP with ENDF/B-V	0.99	0.58	1.33
(ENDF/B-V - ENDF/B-IV) × 100/MCNP with ENDF/B-V	-5.68	-5.09	-4.61
(ENDF/B-V - ENDF/B-IV) × 100/ANISN with ENDF/B-V	-5.60	4.76	-5.59

lithium blanket; b) the lithium blanket generates more energy per fusion neutron relative to the lithium-lead blanket; c) among the possible reflector materials, the carbon reflector produces the highest TBR; d) the high-Z reflector materials (Mo, Cu, W, or steel) generate more energy per fusion neutron and produce smaller TBRs relative to the carbon reflector; e) lithium-6 enrichment is required for the lithium-lead blanket to reduce the total blanket thickness; and f) the energy deposition per fusion neutron reaches a saturation as the blanket thickness, the fraction of the high-Z material in the reflector, or the reflector zone thickness increases (this allows one to design the blanket for a specific TBR without reducing the energy production)

The tritium breeding benchmark calculations show that the uncertainty in the TBR for liquid lithium blankets is about 1% due to nuclear data processing, multigroup treatment, and numerical errors from the transport codes.

The impact of the different reactor design choices on the reactor performance parameters was studied with three-dimensional models based on the STARFIRE reactor model for several cases. The results from this part of the study are the following: a) the impurity control system (limiter or divertor) with a liquid metal coolant (Li or 17Li-83Pb) and vanadium structure have a negligible effect on the TBR; b) For the same material in the impurity control system, the limiter reduces the energy deposition in the blanket by about 3% relative to the divertor; c) the limiter with water coolant and copper structural material causes about a 4% drop in the TBR relative to the lithium-vanadium limiter; d) For the lithium-lead blankets, the drop in the TBR is 19% and 15% for steel-water and steel-helium materials for the inboard blanket, respectively; e) The water-steel inboard blanket produces a 6% increase in the energy deposition per fusion neutron relative to the breeding blanket in the inboard section; and f) The effect of an inboard blanket on the performance of the lithium blanket is slightly moderated relative to the lithium-lead blanket.

References

1. D. L. Smith, et al., "Blanket Comparison and Selection Study - Final Report," Argonne National Laboratory, ANL/FPP-84-1, September 1984.

2. C. C. Baker, et al., "Tokamak Power Systems Study - Fiscal Year 1985," ANL/FPP-85-2, October 1985.

3. W. W. Engle, Jr., "A User's Manual for ANISN, A One Dimensional Discrete Ordinates Code with Anisotropic Scattering," Oak Ridge Gaseous Diffusion Plant, ORGDP-K-1963 (1967).

4. R. W. Roussin et al., "The CTR Processed Multigroup Cross Section Library for Neutronics Studies," Oak Ridge National Laboratory ORNL/RSCIC-37.

5. Y. Gohar and M. A. Abdou, MACKLIB-IV: A Library of Nuclear Response Functions Generated with MACK-IV Computer Program from ENDF/B-IV," *Argonne National Laboratory, ANL/FPP/TM-106 (1978).*

6. J. H. Huang and M. E. Sawan, "Neutronics Analysis for the MARS Li-Pb Blanket and Shield," Journal of Nuclear Technology/Fusion, Vol. 6, No. 2, 883 (1983).

7. M. B. Emmett, "The MORSE Monte Carlo Radiation Transport Code System," Oak Ridge National Laboratory, ORNL-4872 (1975).

8. R. W. Conn, Y. Gohar and C. Y. Maynard," Two-Dimensional Neutron Transport Calculations in a Torus," Transaction of American Nuclear Society, Volume 44, 140 (1983).

9. C. C. Baker et al., "STARFIRE - A Commercial Tokamak Fusion Power Plant Study," ANL/FPP-80-1 (1980).

10. Y. Gohar and M. A. Abdou, "Neutronics Optimization of Solid Breeder Blankets for STARFIRE Design," Proceedings of the Fourth Topical Meeting on the Technology of Controlled Nuclear Fusion, King of Prussia, PA, October 14-17, 1980.

11. Y. Gohar, "Limiter Impact on the Tritium Breeding Ratio in a FED/INTOR Reactor," Trans. Am. Nucl. Soc. 44, 140 (1983).

12. LASL Group X-6, "MCNP - A General Monte Carlo Code for Neutron and Photon Transport, Version 2B," Los Alamos National Laboratory, LA-7396-M, Revised (April 1981).

13. C. R. Weisbin et al, "VITAMIN-E: An ENDF/B-V Multigroup Cross-Section Library for LMFBR CORE and Shield, LWR Shield, DOSIMETRY and Fusion Blanket Technology," Oak Ridge National Laboratory, ORNL-5505 (February 1979).

14. J. H. Huang and M. E. Sawan, "Benchmark Calculations of Tritium Breeding in a Li17Pb-83 Fusion Reactor Blanket," Transactions of the American Nuclear Society, Vol. 44, 142 (1983).

Acknowledgements

The author wishes to acknowledge the assistance of K. Furuta and K. Wenzel during the course of this work.

DISTRIBUTION LIST FOR ANL/FPP/TM-208

Internal:

C. Adams
C. Baker
M. Billone
R. Blomquist
J. Brooks
Y. Cha
Y. Chang
O. Chopra
R. Clemmer
D. Ehst
K. Evans
P. Finn
E. Fujita
E. Gelbard
Y. Gohar (10)
L. Greenwood
D. Gruen
A. Hassanein
T. Hua
C. Johnson
A. Krauss
L. LeSage
Y. Liu
B. Loomis
S. Majumdar
R. Mattas
B. Picologlou
K. Porges
C. Reed
A. Smith
D. Smith
H. Stevens
D. Sze
C. Till
L. Turner
S. Yang
T. Yule
FPP Files (50)
ANL Contract File
ANL Libraries
ANL Patent Dept.
TIS Files (5)

U.S. Department of Energy:

DOE-TIC, for distribution per UC-20 (105)
Manager, Chicago Operations Office
S. Berk, Office of Fusion Energy
M. Cohen, Office of Fusion Energy
R. Dowling, Office of Fusion Energy
G. Haas, Office of Fusion Energy
G. R. Nardella, Office of Fusion Energy
A. Opdenaker, Office of Fusion Energy
T. Reuther, Office of Fusion Energy
P. Stone, Office of Fusion Energy

External:

M. Abdou, University of California, Los Angeles
R. G. Alsmiller, Oak Ridge National Laboratory
J. Anderson, Los Alamos National Laboratory
V. C. Baker, Oak Ridge National Laboratory
S. Baron, Brookhaven National Laboratory
W. Bauer, Sandia Laboratories
L. A. Berry, Oak Ridge National Laboratory
M. R. Bhat, Brookhaven National Laboratory
B. L. Bishop, Oak Ridge National Laboratory
J. A. Blair, Oak Ridge National Laboratory
A. Bolon, University of Missouri-Columbia
L. Booth, Los Alamos National Laboratory
L. Bromberg, Massachusetts Institute of Technology
R. Brown, Los Alamos National Laboratory
S. Burnett, GA Technologies, Inc.
D. Campbell, Oak Ridge National Laboratory
J. Cannon, Oak Ridge National Laboratory
L. Carter, Hanford Engineering Development Laboratory

G. Casini, C.E.A. Ispra (VA), Italy
D. Cohn, Massachusetts Institute of Technology
R. Conn, University of California, Los Angeles
J. Crocker, EG&G Idaho, Inc.
J. Davis, McDonnell Douglas Astronautics Company
S. Dean, Fusion Power Associates
T. Drolet, Ontario Hydro, CANADA
D. Dudziak, Los Alamos National Laboratory
M. J. Embrechts, Rensselaer Polytechnic Institute
B. Engholm, GA Technologies, Inc.
C. Flanagan, Fusion Engineering Design Center/Oak Ridge National Laboratory
H. Furth, Princeton Plasma Physics Laboratory
T. Gabriel, Oak Ridge National Laboratory
J. Garner, TRW, Inc.
N. Ghoniem, University of California, Los Angeles
J. Gordon, TRW, Inc.
D. Graumann, GA Technologies, Inc.
R. A. Gross, Columbia University
G. Haste, Oak Ridge National Laboratory
C. Henning, Lawrence Livermore National Laboratory
G. Hollenberg, Hanford Engineering Development Laboratory
R. Howerton, Lawrence Livermore National Laboratory
S. Iwasaki, Lawrence Livermore National Laboratory
D. Jassby, Princeton Plasma Physics Laboratory
R. J. Juzaitis, Los Alamos National Laboratory
S. Kailas, Indiana University
M. Kazimi, Massachusetts Institute of Technology
A. Klein, University of Oregon
R. Krakowski, Los Alamos National Laboratory
H. Kranse, Max-Planck Institute fur Plasmaphysik, West Germany
A. Knoblock, Max-Planck Institute fur Plasmaphysik, West Germany
L. P. Ku, Princeton Plasma Physics Laboratory
G. Kulcinski, University of Wisconsin, Madison
J. D. Lee, Lawrence Livermore National Laboratory
R. A. Lillie, Oak Ridge National Laboratory
R. Little, Princeton University
R. J. Livak, Los Alamos National Laboratory
G. Logan, Lawrence Livermore National Laboratory
P. Lykoudis, Purdue University
J. A. Maniscalco, TRW, Inc. Redondo Beach
C. Marinucci, SIN, Villigen, Switzerland
C. Maynard, University of Wisconsin-Madison
H. McCurdy, Oak Ridge National Laboratory
G. H. Miley, U. Illinois, Urbana
R. Miller, Los Alamos National Laboratory
R. Moir, Lawrence Livermore National Laboratory
D. Montgomery, Massachusetts Institute of Technology
D. Moyer, Grumman Aerospace Corporation
T. Nakamura, Japan Atomic Energy Research Institute
Y. Oka, University of Tokyo, Japan
S. Pearlstein, Brookhaven National Laboratory
S. Piet, EG&G Idaho, Inc.
J. Powell, Brookhaven National Laboratory
R. J. Puigh, Westinghouse Hanford Company

J. Rathke, Grumman Aerospace Corporation
F. Ribe, University of Washington
R. P. Rose, Westinghouse Electric Corporation
R. Roussin, Radiation Shielding Information Center, ORNL
P. H. Rutherford, Princeton University
P. Sager, GA Technologies, Inc.
R. T. Santoro, Oak Ridge National Laboratory
M. Sawan, University of Wisconsin-Madison
J. Schmidt, Princeton Plasma Physics Laboratory
K. Schultz, GA Technologies Inc.
J. Scott, Oak Ridge National Laboratory
Y. Seki, Japan Atomic Energy Research Institute
T. Shannon, Fusion Engineering Design Center/Oak Ridge National Laboratory
W. Stacey, Jr., Georgia Institute of Technology
M. Stauber, Grumman Aerospace Corporation
D. Steiner, Rensselaer Polytechnic Institute
J. Stout, Oak Ridge National Laboratory
K. Sumita, Osaka University, Japan
D. W. Swain, Oak Ridge National Laboratory
M. A. Sweeney, Sandia National Laboratories
A. Takahashi, Osaka University
K. I. Thomassen, Lawrence Livermore National Laboratory
W. L. Thompson, Los Alamos National Laboratory
A. Tobin, Grumman Aerospace Corporation
T. Tomabechi, Japan Atomic Energy Research Institute, JAPAN
Prof. Vetter, Kernforschungszentrum Karlsruhe und Verwaltung, GERMANY
D. Wattecamps, Commission of the European Communities
G. L. Woodruff, University of Washington
V. Zoita, Central Institute of Physics, Bucharest
Bibliothek, Max-Planck-Institute fur Plasmaphysik, WEST GERMANY
C.E.A. Library, Fontenay-aux-Roses, FRANCE
Librarian, Culham Laboratory, ENGLAND
Library, Centre de Recherches en Physique des Plasma, Lausanne, Switzerland
Library, FOM-Institute voor Plasma-Fysika, The Netherlands
Thermonuclear Library, Japan Atomic Energy Research Institute, JAPAN